



УДК 543.544

Multi-component diffusion mass transfer in bi-functional nanocomposite matrices with the author's model

Kalinitchev A.I.

Institute for Phys. Chem. & El. Chem., Rus. Acad. Sci., Moscow

Поступила в редакцию 23.09.2016 г.

There is presented the generalized theoretical study of the kinetics of the Multicomponent Mass Transfer (MMT) on the basis of the numerical computerized modeling with the elaborated author's new bi-functional Model for the contemporary selective NanoComposite's (NC): r-bead, ro-fiber, or L-membrane matrices.

Keywords: Nano-Composites (NC), mass transfer, selectivity, concentration waves, multicomponent diffusion.

Многокомпонентный диффузионный массоперенос в би-функциональных матрицах нанокompозитов на основе авторских моделей

Калиничев А.И.

Федеральное государственное бюджетное учреждение науки Институт физической химии и электрохимии имени А.Н. Фрумкина Российской академии наук, Москва

В работе представлено обобщенное теоретическое исследование Многокомпонентного Массо Переноса (ММП) на основе численного компьютерного моделирования с решением диффузионных уравнений многокомпонентного материального баланса. Для получения результатов ММП в матрицах современных НаноКомпозитов (НК) различных симметричных форм (г-зерно, го-волокно, L-мембрана) необходимо применение Модели механизма ММП. Такая би-функциональная Модель для НК г,го,L-матриц разработана автором в ряде работ и включает два маршрута для ММП с характеристиками: маршрут I - селективность (K_S) с трансформацией масс, а также маршрут II - $\{D_{i,j,p}\}$, многокомпонентная диффузия.

Для визуализации результатов компьютерного моделирования использован (адекватно воспринимаемый научной аудиторией, и испытанный в течение более 14 лет) авторский метод Научных Компьютерных Анимаций (НКА). «НКАнимация» (т.е. «НКА.avi»-видео файл) представляет собой анимационные фреймы-картинки разноцветных многокомпонентных концентрационных волн, которые распространяются во времени (Т) и в пространстве (г,го,L)-матриц НК.

Ключевые слова: нанокompозиты (НК), массоперенос, селективность, концентрационные волны, многокомпонентная диффузия.

1. Introduction

The aim of this presentation is to consider the generalized theoretical approach including the fundamental aspects of the Multicomponent Mass Transfer (MMT) kinetics in

the various *bi-functional* matrices of the Nano-Composites (NC) on the basis of the author's new *bi-functional* NC Model[1-9]. Two theoretical key concepts are used in the study: (1) Author's new *bi-functional* NC Model for the computerized modeling of the MMT kinetics process with n-components ($n=1,2\dots k$) inside the NC matrices of the various symmetrical shapes: spherical r-bead, cylindrical ro-fiber, or planar L-membrane; (2) The fundamental well-known «Wave concept» (denoted as W^+) of the multi-component X_n (distance; Time)-concentration waves ($n=1,2\dots k$) propagating during time (T) in the *bi-functional* NC r,ro,L-matrices for the MMT kinetic process of the k-component mixture ($n=1,2\dots k$)[1-10].

The MMT process for the n-components of the k-component mixture ($1 \leq n \leq k$) is considered for the case when the appearing, and propagating X_n (distance; time)-concentration waves (profiles) move in the course of time (T) inside the NC matrix from the contact: «NC surface/external solution» into the separate particle of the NC sorbent of the various symmetrical r,ro, or L-shapes. The additional significant explanatory illustrations are represented in Figs.1(a-c, left ; d-f, right).

A number of the explanatory illustrations for the MMT kinetic process in the selective and *bi-functional* NC matrices are presented below (Section 1) with the input $J_{i,p}$ -fluxes of the masses of the n-components (Figs. 1a,d) including the corresponding propagation of the concentration waves: $X_{nr(ro)}$ (L,T), or $X_L(L,T)$ – wave's profiles in Fig. 1b($X_{nr(ro)}$), and Fig. 1e(X_{nL}).

Figures 1(a,d) show visually the input vectorial $J_{(r,L),i,j,p}$ -mass fluxes of the diffusing i,j,p -components with the corresponding $\{D_{i,j,p}\}$ -multiDiffusivities. The directions of the $J_{r,(ro)}$ -vectors are pointed by the vectorial (*radial*) arrows to the central core of the r-bead (or ro-fiber) in Fig. 1a. Figure 1d shows the *horizontal* vectors of the J_L -mass fluxes for the i,j,p -components with the $\{D_{i,j,p}\}$ -diffusivities in the pores of the NC L-matrix through the planar L-membrane.

The every disturbances of the X_n -concentration for the every n-component ($1 \leq n \leq k$) of the k-component mixture generate the propagating $X_{nL(ro)r}(L,T)$ -concentration waves (profiles) during the modeling of the NC or (IE_x) MMT processes in the L;r,ro-matrices. The corresponding $X_{nr,L}$ -concentration waves ($X_{nr(ro)}$ -radial waves (Fig. 1b), or X_{nL} -planar ones (Fig.1e)) are presented schematically in Figs. 1(a,d), and Figs. 1(b,e) correspondingly.

The schematic profiles of the propagating $X_{nr,ro;L}$ -concentration waves inside the NC r,(ro);L-matrices are presented appropriately in Figs. 1(b,e) under Figs.1(a,d) for the cut of the NC L;r,(ro)-matrices. In Figs.1(b,e) the r,(ro)-radial, or L-planar $X_{nr,ro;L}$ -concentration waves travel inside the *bi-functional* NC r,(ro);L-matrices along r(ro)-radius (Fig.1b, radial $J_{ri,p}$, to the r,(ro)-Centers), or through the L-membrane (Fig. 1e, horizontal $J_{Li,p}$; *right to left*).

Thus the $X_{r,(ro);L}$ -concentration waves are shown in Figs. 1(b,e) appropriately under Figs. 1(a,d) for the NC r(ro)-matrices, (Fig. 1a), or L-matrix(Fig. 1d) with the essential discrepancy for the input vectorial $J_{r,L}$ -fluxes in Figs. 1(a,*left* ; d,*right*) where the $J_{r(ro)}$ -fluxes are «*radial*» (Fig. 1a), and the J_L -fluxes are «*horizontal*»(Fig. 1d).

Figure 1c(downstairs, *left*) shows the obvious experimental illustrative SEM micrography of the NC r-bead together with the $X_r^{Cu^{++}}$ -*radial* concentration wave propagating to the r-Center (the experimental *radial* r-wave profile, Fig.1c) in the radial directions of the «white» arrows (1c). Figure 1c illustrates the propagation of the *radial* $X_r^{Cu^{++}}$ -concentration experimental wave with the propagating frontal (Cu^{2+}/Cu^0)-boundary during the oxidation process[11,12].

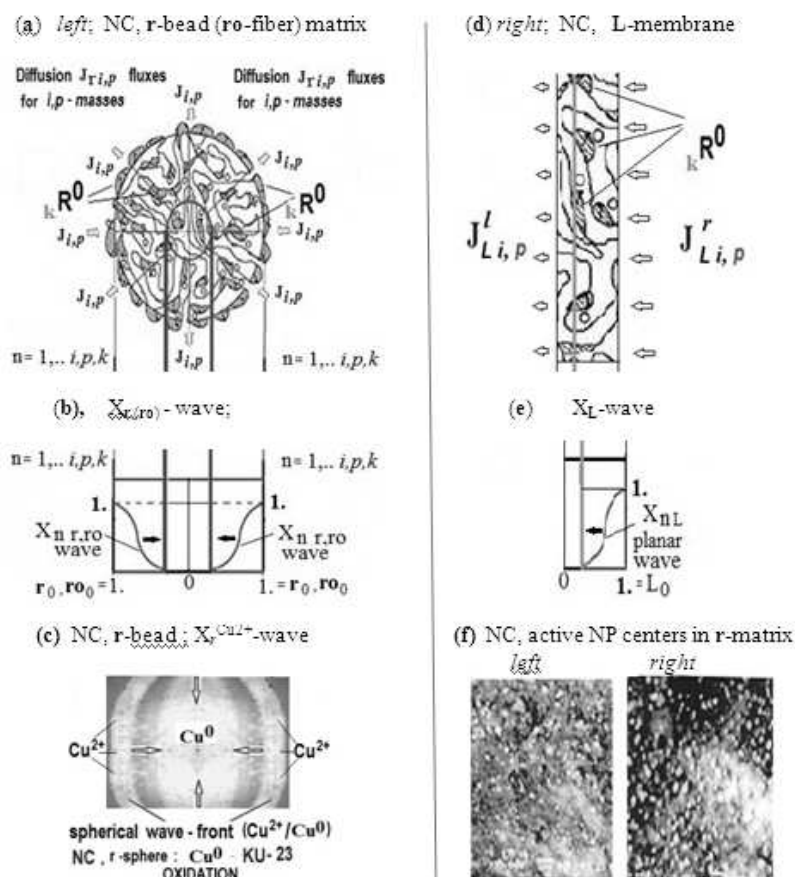


Fig. 1(a-c, left; d-f, right). Illustrations for MMT inside the *bi-functional* NC media (r(ro);L-matrices): (a-c) scheme of cuts of r-sphere, (or ro-cylinder), and L-membrane (d,e) with input $J_{ri,p}$ (a); $J_{Li,p}$ -fluxes(d); active kR^0 -«nanosites» (a,d-shaded); (b,e)- $X_{nr,L}$ -concentration r(ro)-radial, or L-planar waves (along arrows); (c)-experimental SEM micrography of Cu^{++} -radial wave; (NC cut, Me⁰-IEx resin: Cu⁰-KU23); zero charged Cu⁰-nanocenters & «inner part» of the NC r-bead[11,12]; (f)-two experimental SEM micrography of NC, (Ag⁰-KU23 resin) for two r-matrices¹³ where (light dots: kR^0 -active «nanosites») with two various displacing agents: Na₂S₂O₄ (left); N₂H₄, (right).[13] Magnification: 10000. KU23 resin (Russia).

Figures 1f (left, right) demonstrate the SEM micrography with the NP agglomerates embedded into the NC r-matrix synthesized[13]. The corresponding experimental SEM micrography of the synthesized NC represents the two experimental illustrations (1f) of the NP agglomerates (light dots) inside the NC r-matrix[13]. Figures 1f(left, right) show the structures for the NC «Me⁰(Cu⁰)-(KU23 resin)» including zero valent Metal NP (Cu⁰) inside the *bi-functional* NC r-matrix (see also the SEM micrography in the russian monograph[13]).

The time(T)-distance(r,ro;L) behavior of the $X_{nr,ro;L}$ (distance; T)-concentration waves for the n-components ($1 \leq n \leq k$) is calculated by the computerized calculations during the modeling of the MMT, NC kinetics processes. The numerical solutions of the mathematical system of the multi-component partial differential Eqs. (3.3), Section 3 (below) for the MMT inside the various *bi-functional*, and selective NC r,ro;L-matrices (Figs. 1a,d) including the r(ro)-radial, or L-planar $X_{nr(ro),L}$ (T)-concentration waves-profiles are demonstrated in Figs. 1(b,e).

The results of the numerical computerized modeling (described in S.2,3 below) are represented by the propagation of the $X_{nr,L}$ -concentration waves along the distances of the NC r,ro;L-matrices in the course of time (T) (the details are described below, S.3-5). In

addition the interaction (or «interference») of the propagating multicomponent $X_n(r,ro,L; T)$ -concentration waves (X_n -profiles in Figs.1b,e) takes place inside the NC matrices during the MMT kinetics process (S.3-5).

The generalized theoretical study of the MMT kinetics process in the *bi-functional* NC L;r,ro -matrices is realized by the author's numerical computerized modeling. The new theoretical results of the MMT process in the NC medium are derived on the basis of the phenomenological approach of the non-equilibrium thermodynamics[14] by the numerical computerized solutions of the partial differential mass balance n-Eqs (3.3;S.3) for the MMT in the NC sorbents[1-10]. Such way of the computerized modeling of the NC, MMT process should be realized via the corresponding implementation of the authors *bi-functional* Model[1-8] into the system of the partial differential mass balance n-Eqs.(3.3) mentioned (in S.3).

The detailed description of the new author's *bi-functional* NC Model with the two MMT co-working (I&II)-routes (Figs. 2a,b; S.2) expressing agreeably the two properties (I,Selectivity & II,multi-Diffusivities, $\{D_{i,j,p}\}$) are presented for the MMT process in the next Section (S.2). The main characteristics of the author's *bi-functional* Model are published[1-9] and represented visually here via the conceptual illustrations-schemes in Figs. 1(a-f)&2a,b. Figures 2a,b present the author's «*bi-functional* NC Model» concepts in S.2.

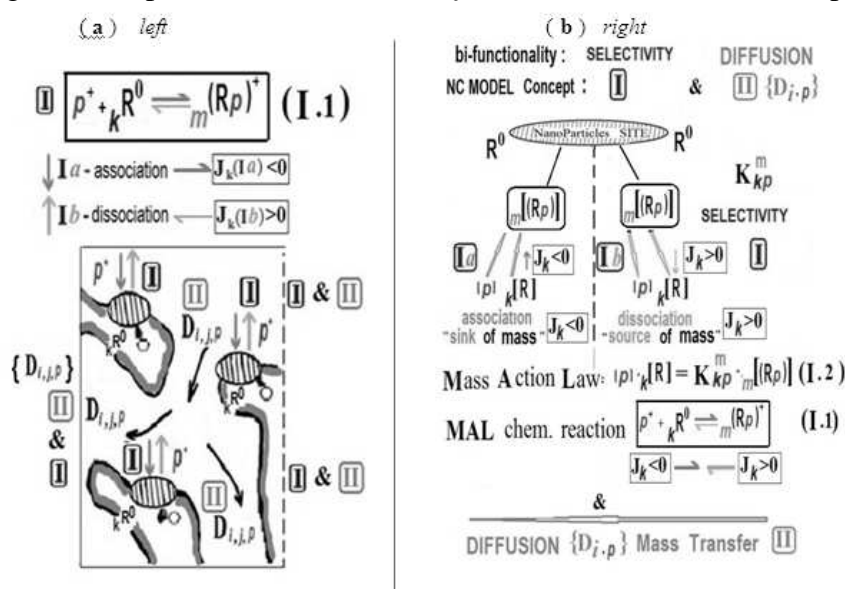


Fig. 2(a,b) Conceptual illustrations of the *bi-functional* NC Model; route I (Selectivity, I) with «mass transformations» MAL relation (I.2) (b); *bi-functional* NC matrix with « ${}_k R^0$ -nanosites» (dashed, a,b); multi-Diffusion co-route II, $\{D_{i,j,p}\}$. Visual scheme of route I (a, up): (Ia)-association; (Ib)-dissociation. (a,b): reaction (I.1); (Selectivity, I & II), multi-Diffusion, $\{D_{i,j,p}\}$ in NC pores, down); «sink»(Ia→)-«source»(←Ib) mechanism (a,b, «left-right») conditioned by Selective route I, MMT. $K_S = K_{kp}^m$ -Selectivity constant in (I.2). The inequalities for J_k -fluxes: $J_k < 0$ (Ia →; a) ; $J_k > 0$ (←Ib ; a,up).

The detailed description of the experimental properties of the new NC *bi-functional* materials with the example: «NC Metal-Ion Exchangers» including the review of the methods of the NC synthesis has been published recently in the Russian monograph[13]. In the monograph the theoretical aspects for the synthesis of the *bi-functional* NC matrices have been discussed in details including a large number of the practical NC applications[13].

The micrography of the experimentally synthesized NC (SEM examples in Figs. 1c,f) is obtained by prof. T. Kravchenko group from Voronezh State University[11-13].

Many experimental samples are presented as the illustrations of the NC media in the monograph including the additional various co-author's joint publications[11-13]. Three illustrations of the SEM micrography are presented here (S.1) in two Figs. 1(c,f)[11-13]. In the monograph there are considered many other experimental illustrations and applications for the synthesis of the NC matrices including the NP (Me^0) agglomerates (Figs. 1f, NP agglomerates –«light dots»)[13]

The NC material includes the numerous NanoParticles (NP) (Figs. 1f) embedded inside the *bi-functional* NC matrix-medium due to the NC synthesis[13]. The details of the NC synthesis with zero valent Metal (Me^0 ,NP) agglomerates in the NC matrices are presented in the monograph[13]

Further in the result of the computerized simulation of the MMT process with the mathematical numerical solution of the n-component MMT system of the partial differential mass balance n-Eqs. (3.3) there are obtained the multicomponent X_n -concentration waves-profiles propagating during the MMT kinetics process in the *bi-functional* NC matrices (S. 2-5). The time (T)-distance (r,ro;L) behavior of the X_n (distance; T)-concentration waves is analyzed and presented by the application of the well-known in science: «wave» concept (named here as the «key» W^+ -concept, S.4-6) in the review[7,8].

The computerized simulation of the MMT is realized via the numerical mathematical solution of the multi-component n-system of the partial differential MMT n-Eqs. (3.3 in S.3) including the implementation of the author's *bi-functional* NC Model (S.3)[1-9].

In the computerized modeling a number of the accompanying relationships is included additionally into the theoretical consideration. The relations are used generally in the irreversible thermodynamics phenomenological approach: classical Nernst-Planck relationship, Mass Action Law (MAL_S), electro-neutrality relationships, and some others (S.3)[14].

The theoretical study of the NC, MMT process with the propagation of the interfering X_n -concentration waves ($1 \leq n \leq k$) is fulfilled via the well-known and widely applicable key wave concept (W^+) mentioned (its short review is in S.4,5)[1-9]. Thus the wave W^+ -concept is the second, general and very effective key conception used for the generalized theoretical investigation of the MMT kinetics processes [1-10]. The first concept of the MMT study: the author's *bi-functional* NC Model[1-9] mentioned is described thoroughly in S.2 (Figs. 2, below). The detailed description of the key wave W^+ -concept for the multi-component ($n \leq k$) mass balance partial differential MMT n-Eqs. (3.3) is observed in this manuscript (S.4,5; see also[1-10]).

The «multi-component X_n -concentration wave», or (W^+)-concept is very effective in the generalized theoretical study[1-10] of the MMT kinetics including the author's *bi-functional* NC Model with the two (I, Selectivity)&(II, multi-Diffusion) co-routes implemented for the MMT process in the NC, L; ro, r-matrices (Figs.2a,b).

The distance(L;r,ro)-time(T) behavior of the propagating X_n (L;r,ro; T)-concentration n-waves (W^+ -concept) in the *bi-functional* NC L;r,ro,r -matrices (S.5) have been demonstrated visually to the sci. audience (at many Int. conferences) for many variants with the well perceivable manner via the computed multi-colored SCAnimations (that is the «SCA.avi» video files) assembled by the author. The details of the «SCA.avi» video files applications are discussed in the Conclusion of the manuscript (S.6.2).

Further the details of the various computerized multi-colored SCAnimations («SCA.avi» video files) which show visually the propagation of the $X_{n,L;r,ro}$ (distance; Time)-concentration waves are discussed purposefully in the final CONCLUSIONS (S.6.2).

After the execution of the author's computer *Fortran* programs the numerical computerized solution of the partial differential mass balance n-Eqs.(3.3) for the MMT kinetics process is presented numerically via the functional time dependence: $X_n(\text{distance}; T)$ concentration waves[2-10]. The results of the computerized calculations for the MMT process are presented as the multi-component numerical computational tables. At this point the theoretical analysis of the multi(n)-component computational tables is impossible directly.

Therefore after the computerized modeling the problem of the multi-«*visualization*» (visual presentations for the any scientific audience[2]) of the numerical results of the theoretical study for the MMT kinetics (and dynamics) should be resolved. In these cases the obtained computerized results might be visualized via the multi-colored visual description of the behavior of the propagating multicomponent $X_n(\text{distance}; T)$ concentration waves[2-10]. The problem of the visualization for the MMT kinetics is solved by the author via the visual method of the mentioned multi-colored «Scientific Computerized Animations («*SCA.avi*» video files) presented for the $X_n(\text{distance}; T)$ dependences for the X_n -concentration waves[2,7,8] at the many all Russian and International conferences (*see* S.6.2).

The author's multi-colored SCAnimations are represented by the video files («*SCA.avi*») which are assembled from the computerized separate «frame-pictures» (for the examples *see* Figs. 4a,b; below in S.5). The frames for the «*SCA.avi*» are prepared by the author on the basis of the numerical results of the computerized modeling calculations. The computerized «*SCA.avi*» video files show visually the propagation of the multicomponent $X_n(\text{distance}; T)$ -concentration waves, naturally multi-colored ones (as in Figs. 4a,b) in the course of time (T) inside the NC L;r,ro-matrices via the easily perceivable SCAManner (*see* the final S.6.2 in Conclusions)[2-10].

Previously the approaches for the various IEx multicomponent kinetic models (though not for the NC ones) had been using during long-time period (for around 50-60 years) starting from early F. Helfferich book[15] through his review[16,17] with emphasizing of the STATE-OF-THE-ART-REPORT[18] till 80-90th[7,8,19-25].

In this manuscript (S.4,5) there are presented the modern new investigations published partly in the previous author's articles[1-10]. The corresponding theoretical results for the MMT kinetics on the basis of the key wave W^+ -concept includes the propagating $X_n(\text{distance}; T)$ -concentration waves behavior in the NC L;r,ro -matrices.

The proposed postulates of the elaborated author's *bi-functional* NC Model give the possibility to include the *bi-functional* nature of the NC matrices (I, Selectivity & II, multi-Diffusion $\{D_{i,p}\}$, Figs. 1a,b; 2a,b) into the theoretical computerized modeling[1-10].

2. Modern author's *bi-functional* NC model, MMT kinetics

The conceptual illustrations of the contemporary author's NC *bi-functional* Model elaborated recently[1-10] are presented in Figs. 2a,b (*below*). The elaborated author's contemporary *bi-functional* NC Model is assigned for the implementation into the computerized numerical modeling of the MMT kinetics process in the *bi-functional* NC r,ro;L-matrices with the detailed explanations given below (S.2, 3, *see* also the author's articles[1-9]).

In the elaborated author's *bi-functional* NC Model mentioned it should be marked especially the introduction of the purposeful «association-dissociation» MAL_S reaction (I.1; I.2) in Figs. 2a,b) realizing the most important property of the *bi-functional* NC Model for the MMT process: the Selectivity one. The conceptual visual illustrations of the *bi-*

functional NC Model are presented in Figs. 2a,b with the *two* co-working (I&II) co-routes in the NC matrix for the MMT kinetic process.

Figures 2a(*left*),b(*right*) show the MAL_S (I.2) relation of the reaction (I.1) with the K_S , (or $K_{k,p}^m$, (I.2))-Selectivity constant (K_S , route I) in the conceptual illustrations. Figures 2a,b(*up*) describe visually the two mass transfer (I&II) co-routes: I-Selective «mass transformation»(*up*) & II-multi-Diffusion, $\{D_{i,j,p}\}$ (*down*) for the MMT process (see Figs.2a,b I & II). The details are presented in the Sections (S.2,3) including the basis of the mathematical computerized simulation via the partial differential mass balance n-Eqs.(3.3).

The $\{D_{i,p}\}$, multi-Diffusion MMT for the i,j,p -components (co-route II, Fig. 2b, *down*) is included into the consideration in the *bi-functional* NC Model together with the property of the Selectivity (co-route I) Figs. 2a,b,*up*). The property of the Selectivity (I) is characterized by the corresponding Selectivity MAL_S factor (I, $K_S=K_{kp}^m$ (I.2); Figs.2b, *up*). The additional multi-diffusion MMT co-process, (II) in the pores of the *bi-functional* NC matrix is characterized by the corresponding multi-Diffusivities, $\{D_{i,j,p}\}$ -factors in Figs.2a,b, II.

Thus the author's theoretical NC Model for the MMT into the *bi-functional* NC $r,ro;L$ -matrices is described by using of the two types of the co-working mass operating routes (I&II), (Figs. 2a,b): mass «transformation»(co-route I), Selectivity MAL_S reaction with k,p,m -components (reactants) together with the multi-diffusion MMT in the pores, co-route II ($\{D_{i,j,p}\}$, multi-Diffusivities of i,j,p -components).

The first step in the creation of the author's *bi-functional* NC Model consists in the deliberate declaration and introduction into the consideration of the specific k -component: kR^0 -«nano-sites» inside the NC matrix (Figs.2a,b,*up*)[1-9]. The kR^0 -«nano-sites» component¹ with zero charge (and variable $[kR^0]$ -concentration) is illustrated visually as the small («dashed») nanosites in Figs. 1a,b, and 2(a,b,*up*).

The fixed, and immovable kR^0 -component (with variable $[kR^0]$ -concentrations and zero k -Diffusivity, $D_k=0$) is introduced deliberately[1-9] following to the theoretical (Figs. 1a,d; 2a,b) and experimental illustrations (Figs.1f, *light* dots) for the active kR^0 -nanosites (experimental NP agglomerates) which are embedded via the synthesis[13] into the NC matrices[1].

The specific kR^0 -component (with the variable $[kR^0]$ -concentration) inside the NC $r,ro;L$ -matrices is well represented and correlated with the theoretical illustrations of the kR^0 -nanosites (Figs.1a,d; Figs 2a,b,*up*, «dashed»). The following Figs. 3a.b; 4a.b (in S.5) represent the corresponding propagating kR^0 -concentration wave (*brown* solids) in the NC $L;r,ro$ -matrices.

It is «implicated» under the $[kR^0]$ -concentration value the average, and integral concentration of the NP agglomerates through the physical infinitesimal small volume of the differential mass-balance n-Eqs. (3.3) ($1 \leq n \leq k$, S.3) like it is applied usually in the theoretical continuum mechanics during the mathematical derivation of the partial differential phenomenological n-Eqs. (3.3) describing the MMT kinetic process (S.3).

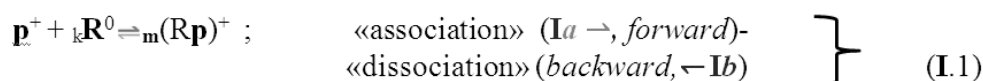
Thus the specific, and fixed k -component, kR^0 -nanosites (with zero diffusivity, $D_k=0$) is declared, and introduced deliberately into the consideration for the theoretical elaboration of the author's *bi-functional* NC Model with the fundamental inclusion of the two co-working mass operating I & II co-routes: (Selectivity, I) & (multi-Diffusion, II) based on the conceptual illustrations in Figs. 2(a,b, I & II co-routes).

The k -component, (kR^0 -nanosites introduced into the consideration) provides the author's NC Model with the additional «degree of freedom» In the result the created *bi-functional* NC Model includes the important, necessary, and key ability: the property of the

Selectivity, (I). It is characterized quantitatively by the MAL_S , K_S -Selectivity parameter described by (I.2) relation (Figs. 2a,b). In the author's *bi-functional* NC Model this property is realized via the I, co-route which is described by the «mass transformation» MAL_S relation (I.2) of the association-dissociation reaction (I.1). The corresponding clear illustration is presented via the conceptual NC schemes in Figs. 2a,b.

For the reaction: $p^+ + {}_kR^0 \leftrightarrow_m (Rp^+)$ (I.1) (Figs. 2a,b) there are realized two stages along the route I: (*forward*), «sorption, $Ia \rightarrow$ » & «desorption, $\leftarrow Ib$ », (*backward*) by the MAL_S «mass transformation» relations (I.1;I.2) (Figs. 2a,b, *up*). In the reaction (I.1) the p,k,m-components (reagents) onto the ${}_kR^0$ -nanosites determine the change of the vectorial $J_{k,p,m}$ -fluxes with the corresponding relations-inequalities for $J_{k,p,m}$ -fluxes via the Selectivity co-route I (Figs. 2a,b, I, *up*). The m,k-components are fixed, and therefore: $D_m, D_k = 0$.

Thus the property of the Selectivity (I) is realized for the MMT process in the NC matrix via the «mass transformation» co-route I (*see* Figs. 2a,b, **I** *up*). During the MMT process the k,m,p-components (reagents) enter into the «association (Ia)-dissociation (Ib)» stages of the reaction (I.1, co-route I) simultaneously, and together with the $\{D_{i,j,p}\}$, multi-Diffusion co-working MMT co-route II (Figs. 2a,b, **II**). [1-8] The two stages are expressed by



$$K_S = K_{pk^m} = \frac{m[Rp]}{[p] \cdot [{}_kR]} , \quad MAL_S \quad (I.2)$$

Further the elaborated *bi-functional* NC Models is implemented into the partial differential MMT n-Eqs. (3.3), (S. 3) via the introduction of the corresponding J_n -mass fluxes along the two co-routes (I&II) consideration: diffusion $J_{i,j,p}$ -fluxes (co-route II), and besides additionally via the introduction of the internal $J_{k,m,p}$ -fluxes (Selectivity co-route, I), (Figs. 1a,d & Figs. 2a,b, **I**, *up* & **II**, *down*) [1-9].

The simulation of the MMT process in the *bi-functional* NC L;r,ro-matrices is executed by the numerical mathematical, and computerized solution of the generalized MMT partial differential n-Eqs.(3.3). The details are presented in S.3 of this manuscript.

The clear conceptual illustration of the author's new, *bi-functional* NC Model is presented in Figs. 2a,b including the change of the various $J_{k,m,p}$ -fluxes in the MMT process [2-9]. It is evident that both m,k-reagents (i.e. the associated $m(Rp)^+$ -complex, m^{th} -component onto the *fixed* ${}_kR^0$ -nanosites) have no $D_{m,k}$ -diffusivities ($D_m=0$; $D_k=0$).

The second ${}_kR^0$ -component (reagent) in the reaction (I.1) is declared earlier (S.2, *above*), and thereafter implemented into the mass balance equations (3.3) via the internal J_k -flux (S.3). The k-component (with the variable $[{}_kR^0]$ -concentration) plays the crucial role in the formation of the Selectivity, via the I, co-route ((I.1), Figs. 2a,b, **I** *up*).

Thus for the MMT kinetics process inside the *bi-functional* NC matrix-medium the two co-working (I)&(II) co-routes (Figs. 2a,b, **I** & **II**) reflect the two simultaneous processes: «mass transformation» & multi-Diffusion during the MMT kinetics. The second (II) additional multi-Diffusion, $\{D_{i,j,p}\}$ co-process occurs in the NC pores with the $\{D_{i,j,p}\}$ -Diffusivities along the second Diffusion co-route II (*see* Figs. 2a,b, **I** *up*) & **II** (*down*) co-routes).

The conceptual illustrations in Figs. 2a,b represent and clarify the properties of the elaborated author's *bi-functional* NC Model with the all accompanying mass transfer elements for the MMT kinetics process [1-9]. The example of the MMT, NC process with the p^+ , ${}_kR^0$, $m(Rp)^+$ -components in the «mass transformation» (I.1) is presented *below* in S.5

including the corresponding MAL_S relation, Eq.(I.2) along the Selectivity I, co-route (Figs. 2a,b, **I**_{up}).

The mechanism of the MAL_S «association-dissociation» reaction (I.1; I.2) equilibrium (co-route I: «association, $Ia \rightarrow$ »- «dissociation, $\leftarrow Ib$ » , Figs. 2a,b, **I**_{up}) retards the whole MMT kinetics process. The dual behavior of the p-component (reactant) capable to the Diffusion ($D_p > 0$) is combined via the two (alternative) possibilities (a) or (b):

(a) p-component is immovable during the «association» stage ($Ia \rightarrow$ forward) when it is fixed (i.e. included into the $m(Rp)^+$ -complex), and

(b) p-component is not fixed, and therefore capable to the Diffusion (with D_p -diffusivity). Then p-component is free and diffusible consequently during the «dissociation» stage of the $m(Rp)^+$ -complex (backward, $\leftarrow Ib$) (Figs. 2a,b, **I**_{route}).

Typical composition of the $\{D_{i,j,p}\}$, multi-Diffusion of the NC kinetics consists of the various types of the n-components considered in the NC, MMT process: i.e. diffusing (i,j,p^+)-ions, fixed $m(Rp)^+$ -complex, and neutral substances such as zero charged and fixed k-component, kR^0 -«nanosites». The example of the various n-components ($1 \leq n \leq k$) of the k-mixture in the MMT process inside the NC matrix (including the specific, fixed k-component, kR^0 -nanosites) are presented in S.5 of the manuscript. In addition there are included into the consideration the two immovable (i.e. fixed kR^0 ; $m(Rp)^+$), m,k -components (reagents) which are aroused as the consequence of the MAL_S «mass transformation» mechanism (I.1; I.2).

The p^+ -component, and fixed, k-component are associated with the formation of the immovable complex: $m(Rp)^+$ -component (see (I.1) in Figs. 2a,b). Here m,k-numbers of n-components ($n=1,..m,..<k$) are represented by the left index to the component's symbols (examples in S. 2-6: kR^0 , $m(Rp)^+$). The created modern author's NC *bi-functional* Model[1-9] discussed here has common points with the preceding approaches published previously[15-25] especially at the end of the last century[20-25] for the selective IEx kinetics.

However, the previous kinetic models[15-25] have been applied theoretically to the IEx kinetic processes, including the cases accompanied by the chemical reactions in the usual *mono-functional* IEx resins (and for the r-beads only)[15-25] but not for the *bi-functional* NC, MMT kinetics in the L; ro,r -matrixes as it is done here.

The approach presented in author's publications[1-10] (including the more detailed description here) has not been applied previously for the contemporary *bi-functional* NC matrices of various L; ro,r -shapes. This conclusion relates especially to the decisive step in the author's *bi-functional* NC Model: the «landmark decision» (for the NC materials) with the introduction into the consideration of the fundamental k-component (new in principle for the NC): kR^0 -nanosites (with the variable $[kR^0]$ -concentrations)[1-9].

The kR^0 -component plays the decisive key role for the *bi-functional* NC Model[1-9]. This introduction of the new, k-component extends the possibilities of the NC Model transforming it into the *bi-functional* one (see above). Besides during the MMT, NC kinetics it is generated the important (and principally new) integral kR^0 -concentration wave which propagates along the L;ro,r -distances in the course of T-time (see Figs. 3a,b; 4a,b, in S.5). The illustrations of the integral propagating kR^0 -concentration wave behavior is presented in the computed Figs. 4(a, small K_S^1 ; b, large K_S^2). Besides it is demonstrated via the corresponding multi-colored computerized «SCA.avi» video files mentioned (S.1). (The SCA animations («SCA.avi») are discussed in S.6.2 of the CONCLUSION).

In contrast to the previous publications[15-25] mentioned above the obtained theoretical results of the extensive general theoretical computerized study for the MMT, NC kinetics on the basis of the author's NC *bi-functional* Model[1-9] are primary and new.

The generalized theoretical results discussed here are obtained for the first time including in addition the consideration of the three various geometric shapes of the *bi-functional* NC matrices: spherical r-bead, cylindrical ro-fiber, and planar L-membrane (Figs.1a,b).

The created new author's *bi-functional* NC Model for the MMT kinetics is effectively applied further for the computerized simulation of the MMT kinetics process inside the *bi-functional* NC matrix of the three various symmetrical *r,ro,L*-shapes mentioned[1-9]. For the illustration of the computerized modeling (in S. 5) there is used the modern *bi-functional* NC matrix: «Me⁰ - Ion Exchanger»[13] as the real example for the author's modern NC *bi-functional* Model applications.

The modern multicomponent author's NC Model with the key *bi-functional* concept: two co-working (I&II)-routes for the NC, MMT kinetics (see the conceptual scheme in Figs. 2a,b) is included successfully and reasonably into the MMT partial differential n-Eqs. (3.3) with the decisive inclusion of the «sink»(Ia→)&«source» (←Ib) mechanism (co-route I, reaction (I.1), Figs. 2a,b,  up)[1-9].

Herewith, the (I), Selectivity effect of the MAL_S relation (I.2) for the «association-dissociation» reaction (I.1) (Selectivity route  in Figs. 2a,b, up) on the kinetic behavior of the *bi-functional* NC, MMT system may be crucial: the whole NC, MMT kinetics rate may be decreased by one or two orders of magnitude. The decisive dependence of the MMT kinetic process on the K_S-factor (=K_{kp}^m, Figs. 2a,b) of the Selectivity, I in the *bi-functional* NC will be demonstrated in S. 5 (5Variant 1, 5-components).

The generalization of the NC, MMT is realized by the inclusion into the consideration of the additional internal J_{k,m}-fluxes on the co-route I (Figs. 2a,b, left-right) which are expressed by the «sink»(forward, Ia→)&«source»(backward, ←Ib) mechanism (Figs. 2a,b,up .

All the computerized calculations with the results of the author's simulation for the n-component X_{nr,ro,L}-concentration «waves» (distributions) are presented below as the distance dependent X_n(distance; T)-concentration waves in the course of T-time (Figs. 1b,e; especially in Figs. 3a,b; 4a,b, in S.5, below).

Herein there is used in the *bi-functional* NC kinetics the another (second) important key W⁺-concept «of the X_{nL(ro)r}-concentration waves» which propagate along the short distances inside the *bi-functional* NC L;ro,r -matrices. The distances are presented by the dimensionless values: *radius* for the r-bead, (ro-fiber), or *thickness* for the L-membrane (0 ≤ L; ro,r ≤ 1) (Figs. 1b,e, and Figs. 3a(L, up),b(ro,r,down) & 4a,b(K_S^{1,2}), S.5).

The computerized numerical calculations during the generalized simulation give the X_n{distance; T^S}-dependence expressed in the discrete (T^S) time moments. Thus the functional dependent X_n{distance; T^S}-wave distributions present the results of the computerized mathematical finite differences solutions of the partial differential MMT n-Eqs.(3.3).

The _kR⁰(or X_{kR})-concentration wave behavior has the integral character as its propagation includes the influence of all the others: 1,..,i,j,..,m,..,p -wave components in the MMT kinetics process. The computerized simulation results for the propagation behavior of the integral _kR⁰(distance; T^S)-concentration wave (*brown, solid* in Figs. 3a(up),b(down)&4a,b(K_S^{1,2})) are presented and discussed in S. 5 of the manuscript.

In addition the corresponding estimations in the NC, MMT kinetics are presented further (S.5, below) by using the integral CM_k;Disp_k-parameters: Center of Mass (CM_{kR}), and Dispersion (Disp_{kR}) of the propagating integral _kR⁰-concentration wave (of «nanosites»).

3. Computerized simulation of MMT kinetics in NC matrices. Generalized MMT partial differential equations

The generalized phenomenological approach is described here (in S. 3) on the bases of the non-equilibrium thermodynamics approach[14] via the partial differential n-Eqs. (3.3), which have been using together with the new author's *bi-functional* (I, Selectivity & II, multi-Diffusivity) NC Model implemented. In Figs. 2a,b (S.2) the conceptual scheme of the NC Model clarifies the details of the *bi-functional* (I, K_S) & (II, multi-Diffusivity, $\{D_{i,j,p}\}$) NC Model which is implemented into the computerized modeling of the MMT process[1-9].

The multicomponent set of the generalized MMT mass balance Eqs.(3.3) are represented mathematically by the nonlinear diffusional partial differential equations with the corresponding additional, Selectivity terms (S_n^m) in the MMT Eqs.(3.3) including the corresponding «mass transformation» $J_{k,m,p}$ -fluxes realized via the Selectivity co-route I (Figs 2a,b).

The nonlinear, and rather complex multicomponent n-system of the partial differential Eqs. (3.3) with the accompanying relations: (3.4-3.10) is executable only by the computerized numerical simulation with the finite differences. Naturally that the corresponding boundary (3.9) and initial (3.10) conditions are introduced into the consideration for the various L; ro, r-matrices of the NC materials for the computerized mathematical solution of the problem, Eqs.(3.2-3.10).

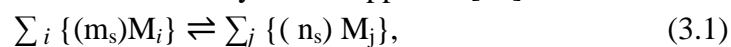
For the generalization of the theoretical results the most appropriate consideration is fulfilled via the dimensionless variables with the $X_n(r,ro,L; T)$ -concentration waves propagating in the course of time (T) along the dimensionless length (r, ro, or L-distances) in the course of the dimensionless T-time.

The mathematical approach is presented in this S.3 with the list of the positions: the equations and relations considered in the computerized modeling of the MMT kinetics inside the *bi-functional* NC matrix containing the kR^0 -nanosites (k-component, Figs. 1a-f; 2a,b)[1-9]. The list includes the association($Ia \rightarrow$)-dissociation($\leftarrow Ib$) MAL_S «mass transformation» reaction (I.1) equilibrium onto the kR^0 -«nanosites» with the phenomenological MAL_S relation (I.2) (Eqs. (I.1; I.2) in Figs. 2a,b; S.2).

The diffusion mass transfer partial differential n-Eqs. include the additional internal terms S_n^m in n-Eqs.(3.3). These S_n^m -terms are described via the internal $J_{k,m,p}$ -fluxes (the conceptual illustration in Figs. 2a(left),b(right)) for the partial differential n-Eqs. (3.3) of the considered multicomponent NC system which are conditioned by the «sink»($Ia \rightarrow$ forward) & «source»($\leftarrow Ib$ backward) mechanism mentioned earlier (route I, with the Selectivity property). Naturally that the total balance for all participating n-substances with the internal $J_{k,m,p}$ -fluxes ($1 \leq m,p \leq k$) is maintained during the computerized numerical simulations by the implicit finite difference technique with the inclusion of the author's *bi-functional* NC Model (S.2, conceptual scheme in Figs. 2a,b) for the L;ro,r-matrices considered (S.2)[1-9].

3.1 Dissociation-association MAL reactions. Mass transformations onto the kR^0 -nanosites

The association-dissociation reactions (similar to (I.1), S.2) may be recorded in the well-known general form on the irreversible thermodynamics approach[14]



where $M_{i,j}$ are the symbols of the i,j -components participating in the «association-dissociation» reaction (I.1) included in the created modern *bi-functional* NC Model postulates ((I.1;I.2), Figs.2a,b; S.2)[1-9]. In correspondence with the MAL generalized reac-

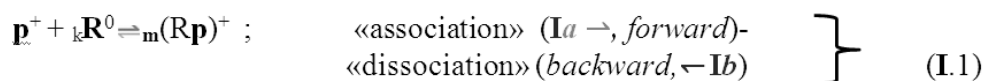
tions (3.1) the generalized MAL_S «mass transformations» Eqns. (3.2) (corresponding to the I route in the NC *bi-functional* Model, Figs. 2a,b, *up*) bring the redistributions of the masses of the participating m,p,k-components which enter into the «association»(sorption)-«dissociation»(desorption) reaction (I.1). For the further advance of the *bi-functional* NC Model considered here the equilibrium of the chemical reactions, Eqns. (3.2), (the route I, considered in Figs. 2a,b, *up*) have been taken into the consideration by using the classical MAL_S relationships[14,17-23,25]

$$\prod_i \{ [X_j]^{ms} [X_i]^{ns} \} = K_S, s = 1, 2, \dots (MAL_S), m_S, n_S \quad (3.2)$$

where the expression $\prod_i (i \neq j)$ is the product of the dimensionless concentrations $\{ [X_j]^{ms} (i=1,2,\dots) \}$; n_s, m_s (negative or positive) are the stoichiometric coefficients of the chemicals in the reactions; s - is the corresponding index. The particular (specific) case of the MAL_S relation (3.2) is presented here by the partial case: MAL_S (I.2) relation in Figs. 2a,b, *up* (S.2) and then in S.3 (*below*).

In principle the stoichiometric coefficients (m_s, n_s) for the MAL_S chemical reactions equilibrium, Eqns. (3.2) might be fractional[2-9,21]. During the computerized simulations[2-9] all the m_s, n_s values are assumed to be (± 1). However in need, all these values may be easily used in the contemporary *bi-functional* NC Model[2-9], as fractional, or more than one (unity).

The particular case of the general MAL_S Eqns. (3.2) used here for the author's contemporary *bi-functional* NC Model has the simple form (in (I.1), (I.2) relations) , Fig. 2a,b



$$K_S = K_{pk}^m = \frac{m[\mathbf{Rp}]}{[\mathbf{p}]^m [\mathbf{kR}]^n}, \quad MAL_S \quad (I.2)$$

with the corresponding Selectivity MAL_S relation (I.2) presented in the conceptual illustrations (Figs. 2a,b, *up*, route I). The MAL_S, K_S -Selectivity constant of the chemical reactions equilibrium (I.1) is depended on the rates of the «association»(Ia \rightarrow ,forward)-«dissociation» (*backward*, \leftarrow Ib) stages (Figs. 2a,b; S.2).

The MAL_S reaction equilibrium of Eq.(I.1) onto the NC, \mathbf{kR}^0 -nanosites (route I, Figs. 2a,b) are introduced mathematically in the n-Eqs. (3.3), (S. 3.3) by the corresponding internal J_k, J_m, J_p -fluxes (Figs. 1a,d; 2a,b) for the MMT process. The resulting phenomenological mathematical description of the MMT process in the *bi-functional* NC L; ro,r-matrices is deduced with the implementation into the mathematical consideration of the created author's *bi-functional* NC, MMT Model[1-9].

The modern approach with all mentioned postulates and equations of the created contemporary author's *bi-functional* NC Model[1-9] has been realized by the computerized numerical modeling. The numerical solution of the multicomponent generalized partial differential MMT n-Eqs. (3.3) mentioned together with the corresponding boundary and initial conditions (Eqns.(3.9), (3.10)) has been applied (via the finite differences) for the computerized modeling with the numerical calculations of the propagating $X_n(r,ro,L; T)$ -concentration waves mentioned (by using the key wave W^+ -concept for the *visualization*[2], see S.5,6).

The numerical technique is based on the implicit finite difference formulation (with the sweeping procedure) for the generalized parabolic partial difference diffusion n-Eqs. (3.3) with the iteration technique including the multicomponent (mathematical) matrix calculations approach, and the multicomponent (mathematical) matrix inversions[2-9,14,21].

The set of the author's corresponding computer *Fortran* programs has been composed for the simulation of the various MMT, NC kinetics processes in the n-component systems.

The $X_n(\text{distance}; T^S)$ -waves behavior is the result of the computer simulation via the elaborated *Fortran* programs for the propagation of the multicomponent $X_n(\text{distance}; T^S)$ -concentration waves along the $L;ro,r$ -distances in the course of the discrete T^S -time[2-9].

The behavior of the multicomponent NC, MMT systems are described effectively on the basis of the conceptual wave W^+ -approach describing the multicomponent propagating waves with $X_{n,(i)L,ro,r}(T)$ -concentration profiles in the NC matrices. (In S.6 there is considered the nonselective IEx MMT kinetics as the partial case of the generalized NC, MMT process).

The NC MMT approach is in the connection with the framework of the various considerations based on the wave W^+ -concept. Previously the multicomponent «wave» theoretical approach has been used especially effectively for the dynamic (chromatographic) systems[26-36].

Thus, the computerized investigations of the NC, MMT kinetics with the influence of the MAL_S (K_S -Selectivity) parameter (I.2) of the reaction (I.1) (route I, K_S or K_{pk}^m ; Figs. 2a,b) have been realized in cooperation with the co-working multi-Diffusion influence (co-route II with the $\{D_{i,j,p}\}$ -Diffusivities) in the pores of the matrices for the i,j,p - components. The MMT, NC kinetics inside the various *bi-functional* NC matrices (Figs. 2a,b) are investigated for the NC of the three symmetrical shapes: L-membrane, ro-cylinder, r-sphere (illustrated in Figs. 1(a-f)). There are included into the consideration the new properties of the elaborated *bi-functional* NC Model[1-9] with using the effective key wave W^+ -concept.

The mathematical realization of the multicomponent Diffusion ($D_{i,j,p}$) NC kinetics, together with the relations for the chemical MAL_S reactions equilibrium, Eqs. (I.1;I.2) are based on the approach of the modern *bi-functional* NC Model (conceptual scheme in Figs. 2a,b). As it is marked above (*here* in S.3) there are no difficulties in the generalization of the MAL_S reactions according to the generalized MAL_S relations (3.2) (*see above*).

Besides there is used the same simple relation for the MAL_{ij} ij -reaction in the pores of the *bi-functional* NC matrix including the arbitrary i, j , ij -diffusing components with the concentrations: $[i]$, $[j]$, $[ij]$. The corresponding simple scheme in the NC pores used for the simple reaction: $i + j \rightleftharpoons ij$ is represented by the simple MAL_{ij} relations for the monovalent components: $[i]*[j] = K_{ij}*[ij]$. The results of the computerized modeling demonstrate that the simple reaction: $i + j \rightleftharpoons ij$ (in the NC pores) don't influence the effect of the *bi-functional* NC Model with the main Selectivity property (co-route I in Figs. 2a,b)[7-9]. Therefore (as it is shown in the results of the computerized modeling)[7-9] the influence of the MAL reaction (in the NC pores): $i + j \rightleftharpoons ij$ is in minority and will not be considered further.

Nevertheless the influence of the minor MAL_{ij} (K_{ij}) reaction ($[i]*[j] = K_{ij}*[ij]$) is also included in the author's computer *Fortran* programs with its introduction in all samples of the mathematical modeling. The results of the computerized simulation show that the influence of the MAL_{ij} reaction (with the K_{ij} -constant) is not essential (in comparison with the K_S -Selectivity effects) in all the computed cases[7-9].

In the theoretical discussion of the MMT process in the *bi-functional* NC Model the behavior of the p-component should be noted separately. For the p-component in the *bi-functional* NC matrix it is realized the specific case of the combined «dual» behavior of the diffusible p-component, $D_p > 0$ (*see* S.2). During the MMT process it is transformed

permanently into the fixed $m(\text{Rp})^+$ -complex (*forward, Ia* → & *backward, ← Ib*) via the reaction (I.1) for the «association-dissociation» stages (Figs. 2a,b,up).

In the $m(\text{Rp})^+$ -complex state the p-component is fixed as there are zero diffusivities for the both fixed k,m-components (i.e. fixed k&m-components give $D_k, D_m=0$). So there is the dualism in the p-component behaviour: *free* p-state during the dissociation (*Ib*) stage, and reverse: *fixed* p-state in the $m(\text{Rp})^+$ -complex due to the association (*Ia*) of the $m(\text{Rp})^+$ -complex (I.1) (S. 2, Figs.2a,b).

Meanwhile due to the such specific dualism for p-component behavior it participates in the MAL_S association-dissociation transformation (I.1) $(p^+) \rightarrow m(\text{Rp})^+$, together with the following «transformation»(I.1) of the m,p,k-«masses», (see Figs. 2a,b). It will be shown (S. 5) that due to the («*forward*»*Ia* →)&(← *Ib* «*backward*») p-component «transformation» (I.1) onto the kR^0 -“nanosites” (Figs. 2a,b) the two formed $m(\text{Rp})^+, kR^0$ -concentration waves propagate in the *bi-functional* NC matrix (though k,m-Diffusivities are zero: $D_{k,m}=0$, see Figs. 4a,b($K_S^{1,2}$), S. 5) with the propagating sR^0 -concentration wave, *brown* solids).

In this manuscript the $X_{nL,ro,r}$ -concentration waves behavior (on the basis of the W^+ -concept) is presented for the multicomponent diffusion NC, MMT kinetics including the property of the NC Selectivity (co-route I, Figs.2a,b). The difference and similarity in the concentration waves behavior between the two kinds: of the *dynamic* (in chromatography), and NC *kinetic* systems is described in S.5 (Table 1), and in S.6(Conclusions)[7,8].

In the excellent monograph[26] the dynamic behavior of the X_n -concentration waves in the chromatographic column (filters) is described in the multicomponent chromatographic, and ideal dynamic systems. In such ideal cases (without the dispersion factors in the chromatographic filters) the problem is considered for the dynamic X_n -concentration waves with the multicomponent competitive Langmuir sorption or IEx isotherms for the constant separation coefficients[26,28,32-34].

The mathematical theory of the hyperbolic partial differential equations with the application of the mathematical h-transformation approach (or in other mathematical terminology-Rieman invariants) is effectively used by authors[26] for the description of the propagation of the multicomponent ideal X_n -concentration waves (on the basis of the wave concept)[26].

The visual X_n (distance; T)-concentration kinetic waves behavior (with the example: s Variant 1, $k=5$, in S.5) for the NC, MMT kinetics process including the waves interferences are presented in S.4,5 on the basis of the theoretical computerized simulation for the multicomponent Diffusion $\{D_{i,j,p}\}$ *bi-functional* NC kinetics (in S.5).

3.2 Main Mathematical Formulation with Partial Differential MMT, NC Equations

The kinetic X_n (distance; T)-concentration waves are generated with the subsequent propagation along the short distances: r,ro -radius (or L_0 -thickness) inside the *bi-functional* NC matrices in the course of time (T) during the multi-Diffusion $\{D_{i,j,p}\}$ NC, MMT process.

The multicomponent diffusion $X_{nL,ro,r}$ (T)-concentration waves with their propagation (along $L;ro,r$ -distances), and the interference of the $X_{nL,ro,r}$ (T) -waves inside the *bi-functional* NC $L;ro,r$ -matrices play the decisive role in the description of the diffusion MMT, NC kinetics process. Therefore additionally to the short review *above* this well-known and widely used «wave» approach (*here*, wave W^+ -concept) in the multicomponent NC, and IEx systems[1-10,19-23,25-36] is shortly considered in S. 4, *below*.

The extended ability of the NC materials is specified by the *bi-functionality* of the NC $L;ro,r$ -matrices (see the conceptual s Figs. 2a,b with the two combined I,II-co-routes).

Naturally that the multicomponent diffusion $X_{nL(ro)r}(T)$ -concentration waves may propagate in the pores of the usual IEx medium due to the such driving forces as the concentration gradients with the additional effect of the general electric field gradient ($\text{grad } \Phi$) in Eqs.(3.4) with the $\{D_{i,j,p}\}$ -coefficients as the multi-Diffusion factor (see Eqs.(3.6, 3.7) for the nonzero n-Diffusivities, $D_n > 0$, (however, with keeping in mind, that $D_k, D_m = 0$).

For the MMT, NC kinetics there is one identifying feature concerning propagation of the $X_{nL(ro)r}(T)$ -concentration waves in the *bi-functional* NC L;r,ro-matrices[1-10]. Due to the «mass transformation»: the «sink&source» mechanism (Figs. 2a,b, route I, Eqn. (I.1)) the fixed k-component in the NC matrix: ${}_kR^0$ -«nanosites» will be included into the transformation by MAL_S (I.1; I,2) relations into the another m-component ${}_m(Rp)^+$ in the NC *bi-functional* matrix (see Figs.2,a,b in S.2) with the corresponding change of the ${}_kR^0$ -concentration. Therefore in the result of the «mass transformation» Eqs. (I.1; I.2) the ${}_kR^0_{L(ro)r}$ -concentration wave is changed permanently and propagated along the distances (L;ro,r) in the NC matrices (the examples are presented visually in Figs. 3a,b&4a,b in S.5 below).

Such propagation of the integral ${}_kR^0_{L(ro)r}(T)$ -waves (though with the fixed k-component, $D_k=0$) represents the feature of the NC, MMT kinetics (see the Table 1 & S.6, Conclusions). Thus the two various ${}_kR^0_{L(ro)r}(T)$ & ${}_m(Rp)_{L(ro)r}(T)$ -concentration waves propagate along L;ro,r-distances really (via the «mass transformation» mechanism (I.1) of the Selectivity I, co-route inside the NC matrix for the MMT kinetics process. The details are explained visually in S.5 for the 5-component example: *5Variant 1*.

The propagation of the ${}_kR^0_{L(ro)r}(T)$ & ${}_m(Rp)_{L(ro)r}(T)$ -concentration waves in the course of T-time for the NC, MMT process is demonstrated visually for *5Variant 1*, below (Figs. 4a,b ($K_S^{1,2}$) in S.5). The mass transformations via the route I with the Selectivity property including the influence of the «sink (Ia)-source (Ib)» mechanism (Figs. 2a,b) enrich and complicate the multicomponent diffusion ($D_{i,j,p}$) MMT kinetics process in the *bi-functional* NC L;r,ro-matrices.

As it was mentioned earlier the «sink (Ia) -source (Ib)» mechanism is implemented due to the introduction of the additional internal J_k, J_m, J_p -fluxes terms (see (3.3) n-Eqs., and Figs.1a,d&2a,b) describing decrease of a mass (with negative term $J_k < 0$ for the «sink») or increase of a mass (with the positive term $J_k > 0$ for the «source», Figs. 2a,b)[1-9].

The detailed description of the MMT kinetics by the MMT n-Eqs. (3.3) with the corresponding relationships (3.4-3.10) is given below. According to the MMT diffusion kinetic partial differential mass balance n^{th} -Eqs. ($n = 1, m, i, j, p, \dots k$) (including the additional S_n^m -terms) in the course of T-time with the L;r,ro,r-distances are usually presented in generalized form as follows[1-9,14,21]

$$\frac{\partial X_n}{\partial T} = \underbrace{-\text{div}\{J_n\}}_{\text{[Diffusion term, III route]}} + \underbrace{S_n^m}_{\text{(Selectivity term, I route)}} \quad n = 1, m, i, j, p, \dots k \quad (3.3)$$

Change of n-mass

The NC kinetics MMT partial differential n-Eqs. (3.3) have the mathematical distinctions which in respect to the various NC matrix shapes (r-sphere, ro-fiber; L-membrane) are conditioned in the distinct mathematical expressions for the differential operators: $\text{grad}_{r,ro,L}(X_n)$, and $\text{div}_{r,ro,L}\{J_n\}$. The rather simple physical sense of the generalized MMT n-Eqs. (3.3) is explained and illustrated visually in author's publications[7-9].

The additional S_n^m , terms in Eqs.(3.3) are expressed via the internal J_k -fluxes (co-route I) reflecting the mechanism of «sink»(Ia \rightarrow ; $J_k < 0, J_p < 0, J_m > 0$) & «source»(\leftarrow Ib; $J_k > 0, J_p > 0, J_m < 0$) in Figs. 2(a,b, with I&II co-routes).[1-9] The «sink»-«source» mechanism ex-

presses «mass transformation» of the corresponding k,p,m-components (*see* the conceptual *bi-functional* scheme in Figs. 2a,b).

Besides in the computerized simulation[2-9] there are used the fundamental Nernst–Planck n-relationships (3.4) for the diffusion vectorial $J_{p,i,j}$ -fluxes in the n-Eqs.(3.3) for the each diffusing i,j,p -components with the constant multi-Diffusion coefficients: $\{D_{i,j,p}\}$ - Diffusivities. The classical Nernst-Plank relationship for the $J_{i,j,p}$ -fluxes of the i,j,p -components[10-22] describes the diffusion not only for the charged i,j,p - components but for the not charged one ($z_j=0$) also:

$$J_e = J_e^X + J_e^{el} = -D_e \{ \text{grad } X_e + (F/RT) z_e X_e \text{ grad } \Phi \}, e = i,j,p \quad (D_k=D_m=0) \quad (3.4)$$

where J_e are fluxes for the multi-Diffusion of the e -components (with $\{D_{i,j,p}\}$ -diffusivities; $D_{i,j,p} > 0$).

The Diffusion J_e -fluxes (3.4) (Figs.1a,d) for the e -components are composed from the two characterizing terms: (a) J_e^X is the vectorial flux with the driving force conditioned by the X_e -concentration gradients ($-D_e \text{ grad } X_e$), and (b) J_e^{el} is the additional vectorial flux with the driving force conditioned by the electrical potential (Φ) gradient: $-D_e(F/RT) z_e X_e \text{ grad } \Phi$.

Due to the $\text{MAL}_S(\text{I.2})$ reaction (I.1) (co-route **I**), Selectivity, Figs. 2a,b) the p-component forms the ${}_m(\text{Rp})^+$ -complex with the ${}_k\text{R}^0$ -nanosites mentioned earlier. Therefore the corresponding diffusion $J_{k,m}$ -fluxes are absent: $J_{k,m}=0$, though nevertheless the propagation of the X_k, X_m (distance; T)-waves exists in the NC matrix (*see* the visual example in Figs. 4a,b ($K_S^{1,2}$) in S. 5).

In result the classical Nernst-Plank relations (3.4) together with the second S_n^m - term in the MMT partial differential n-Eqs. (3.3) describe the diffusion MMT for the all n-components. The second additional S_n^m -term in Eqs. (3.3) is conditioned by the «mass transformation» (I.1) reaction (with the $K_S(=K_{kp}^m)$ -Selectivity factor, (I.2)) participating in the NC, MMT kinetics (Figs. 2a,b).

The movement of the propagating ${}_k\text{R}^0_{L(\text{ro})r}(\text{T}) \& {}_m(\text{Rp})_{L(\text{ro})r}(\text{T})$ -concentration waves exists really due to the combined behavior of the p-component (*see* earlier in S.2) with its participation in the Selectivity reaction (I.1) together with two others components (with $[_m(\text{Rp})^+], [_k\text{R}^0]$ -concentrations) in the reaction (I.1; I.2) (*see* Figs. 2a,b).

Thus the interesting phenomena take place during the MMT, NC kinetics (marked in Table 1): the two ${}_k\text{R}^0_{L(\text{ro})r}(\text{T}) \& {}_m(\text{Rp})_{L(\text{ro})r}(\text{T})$ -concentration waves propagate in the NC matrix though the corresponding diffusivities are absent ($D_{k,m}=0$). The reason of this effect is conditioned by the combined behavior of the p-component (*see* above in S. 2,3.).

The material balances in n-Eqs. (3.3) for the multicomponent kinetic NC system should be supplemented by the two additional conditions: for the electroneutrality condition

$$\text{SUM}_n (z_n X_n) = 1, \quad (3.5)$$

for the condition of the absence of the electric current

$$\text{SUM}_n (z_n J_n) = 0 \quad (3.6)$$

The NC (and IEx in S.6) systems described by the Eqs. (3.1)-(3.6) may include a various n-components: i -ions, m-complex, neutral substances including especially (zero charged specific k-component, ${}_k\text{R}^0$ -nanosites), and in addition the ${}_m(\text{Rp})^+$ -component with the charged, but not diffusing (i.e. fixed), (as the diffusivity $D_k, D_m=0$, *see* above, S. 1-3).

As usual, due to the known algebraic transformation the influence of the gradient of the electric field ($\text{grad } \Phi$) is expressed mathematically[14,21] via the sum of the other X_n -concentration gradients by using the absence of the electric current relationship (3.6)[1-10]. Then in the result the J_n -fluxes ($n=1,2,\dots$) are described by its own gradient ($\text{grad } X_n$) with the addition of the multicomponent superposition of X_i -concentrations gradients (grad

X_i) (3.4),(3.7)[1-10,14,17-23]. Such well-known superposition of the gradients (3.7) obtained by this method of exclusion is called the «diffusion potential» in the theory of the irreversible thermodynamics[14]

$$-(F/RT) \text{grad } \Phi = \text{SUM}_i (D_i z_i \text{grad } X_i) / \text{SUM}_i (D_i z_i^2 X_i), \quad i=1,2,\dots \quad (3.7)$$

The fundamental Nernst-Planck relationships (3.4) reflect the dependence of the J_n -fluxes from the concentration gradients together with the integral co-influence of the electric field gradient, ($\text{grad } \Phi$), Eqn.(3.7).

The relationship (3.7) gives the possibility to eliminate formally (mathematically) the gradient of the electric potential (Φ) from the mathematical consideration[14-21] by using the two (3.5), (3.6) relationships, with the final result

$$J_e = J_e^X + J_e^{\text{el}} = -D_e \{ \text{grad } X_e + \text{SUM}_i (D_i z_i \text{grad } X_i) / \text{SUM}_i (D_i z_i^2 X_i) \} \quad (3.8)$$

In result the first term J_e^X in the Eq. (3.8) is conditioned by the individual diffusion D_e of the e -component, and the second J_e^{el} summand represents the influence of the electric field gradient ($\text{grad } \Phi$). Thus the second term in Eq.(3.8) shows the interferences of the X_i -concentration waves propagating in the *bi-functional* NC matrix due to the common electric field (Φ is the electric potential).

For the computerized solution of the MMT, NC (&IEx in S. 6) system the problem should be completed by the accounting of the boundary (3.9) and the initial (3.10) conditions:

$$\begin{aligned} \text{boundary } (r_0, ro_0, L_0 \text{ and } r, ro, L \rightarrow 0) \text{ conditions at } r_0, ro_0, L_0 = 1; X_n = X_n^0, \\ \text{and at } r, ro, L \rightarrow 0; r^2 (\partial X_n / \partial r) \rightarrow 0; ro (\partial X_i / \partial ro) \rightarrow 0; (\partial X_i / \partial L) = 0 \quad (3.9) \\ \text{initial conditions : at } T = 0; X_n = X_n^{00} \quad (3.10) \end{aligned}$$

The electro-neutrality condition (3.5) should be fulfilled also for the boundaries: $r_0, ro_0, L_0 = 1$, or 0 (3.9), as well as at the initial ($T=0$) conditions (3.10).

The obtained results of the computerized simulation (S.5) on the basis of the created modern author's *bi-functional* NC Model (conceptual scheme in Figs. 2a,b) with the MMT n-Eqs.(3.3) are presented via the well-known, key «multi-component concentration waves» W^+ -concept mentioned[2-9]. The short review of the description of the wave W^+ -concept with its applications is presented below in the S.4.

4. Concentration wave W^+ -concept in the multicomponent *bi-functional* NC, MMT kinetics

The obtained results of the computerized simulation on the basis of the created author's contemporary multicomponent *bi-functional* NC Model[1-9] are presented via the well-known multicomponent «concentration waves», W^+ -concept[17-19,21-23,25-39].

The X_n (distance; T^S)-concentration waves arise and propagate along the distance (r, ro)-radius, or L -thickness; dimensionless) inside the NC $L; ro, r$ -matrices during the MMT kinetics process. The multicomponent X_n (distance; T^S) waves with their propagation in the *bi-functional* NC matrix play the decisive role in the description of the MMT, NC kinetics (S. 5). Therefore this well-known and widely used «wave» W^+ -approach (especially in the theory of multicomponent chromatography)[26-36] is shortly reviewed *below* including the next S. 4.1.

The key wave W^+ -concept of «multicomponent waves» is widely used in the theoretical description for many scientific fields of the MMT for various kinetic and dynamic systems. The «multicomponent waves» W^+ -concept has wide area for the applications in such research fields, as percolation processes[26-32], mechanics of liquids, gas dynamics[37], theory of burning and even street traffic[32,33,38,39]. The term «wave» (here,

W⁺-concept) has been used in all these publications[1-10,17-20,22,23,25-36] including the mentioned excellent monograph[26], and the books[32,37-39] concerned with shock waves, car traffic, and kinematic waves. There are phenomenological concepts potentially common to all filtration processes, which can also be extended to a whole series of migration phenomena such as chromatography, sedimentation, electrophoresis and some others[26-39].

The review[34] and additionally the presentations[35,36] published by author in cooperation with W. Hoell (Karlsruhe Res. Center, Germany) include the application of the wave concept in the multicomponent dynamics (chromatography) with the description of the SCT (Surface Complexation Theory) Model. The SCT-Model for the multicomponent IEx equilibrium had been elaborated by prof. W. Hoell group at the end of the last century (see Refs. in the review[34]).

In this manuscript the described postulates of the mathematical modern NC *bi-functional* Model created (S.2, Figs. 2a,b), and MAL_S relations for the chemical reactions equilibrium[1-9] have been implemented into the mathematical description of the MMT,NC kinetics process together with the all relationships including the mass balance partial differential n-Eqs (3.3), electro-neutrality condition (3.5), classical Nernst - Plank equations (3.4) for the J_n fluxes of the n-components (S.3).

All the computerized calculations have been obtained by using the dimensionless values, including X_n-concentrations; D_n-diffusion coefficients; K_S-constants of chemical association-dissociation MAL_S reactions (I.1; I.2). The MMT kinetics in the *bi-functional* NC Model include the multicomponent X_n-concentration waves propagation along the dimensionless distance: L,(ro),or r in the course of the dimensionless time (T=D₀t/r²)[1-9].

4.1 Coherence state of the multicomponent X_n-concentration waves

The coherence conditions for the X_n-concentration waves define a special regime in the propagation of the multicomponent concentration waves in the chromatographic, dynamic systems in which all the X_n-concentration waves of the n-components mixture move synchronously[26]. The concept of the coherence describes the states of the chromatographic systems which they tend to attain similarly to the way that closed system tend to a state of equilibrium, while open system with a fixed boundaries and constant boundary conditions tend to attain stationary states[26-33].

The concept of coherence was developed, and generalized by F. Helfferich[27-30]. This concept makes it possible to treat qualitatively, and to calculate in principle quantitatively the multi-component concentration waves in a chromatographic systems under the arbitrary initial and boundary conditions. On the D. Tondeur opinion[29,30], «the coherence is one of the most deep reaching and powerful concept in process dynamics, at least as far as the multicomponent systems are concerned»[30].

More generally coherence is considered as a state or a rather dynamical regime toward which a dynamic system will naturally tend when relaxing after a finite time[26-30]. However, coherence not only refers to the end state of relaxation after a perturbation but also to the relaxation occurs the way in which an incoherent perturbation breaks up into the coherent modes[27].

The global concept of coherence[26-30] indicates the direction in which the development of the multicomponent system advances towards the final coherent state. The coherence definition with its physical sense has been explained by F. Helfferich clearly[27].

4.2 Interference Effects for the multicomponent X_n-concentration waves

Previously the multicomponent W⁺-concept (for the X_n(distance; T-time)-concentration wave) has been considered not only for the NC, MMT *kinetics* mass transfer[1-9] (see this manuscript) but for the mass transfer *dynamics* in the sorption, and Ion

Exchange (IEx) systems also (sometimes even with the good results)[26-36]. Therefore the propagating multicomponent $X_{ndistance}(T)$ -concentration waves with the key wave W^+ -concept should be considered. It should be stressed as one of the main feature of the MMT, NC kinetics in this manuscript (in S.5 & S.6).

The difference between the propagation of the multicomponent $X_{ndistance}(T)$ -concentration waves in the *kinetics* and *dynamics* of the MMT systems is rather evident though the travelling multicomponent $X_{n(i)distance}(T)$ -concentration waves are originated in both cases. However in addition, there are the essential differences for the comparing of the $X_{n(i)distance}(T)$ -concentration waves behavior in the IEx MMT *dynamics* and *kinetics* systems:

a) In the IEx *dynamics* systems, as a rule, the travelling concentration waves (especially in the theory of the multicomponent chromatography[26]) used to reach the stage named as «coherence» (which is introduced by F. Helfferich[27]). This important generalized concept is discussed in many publications[26-33] (*see also above* here). In this case the linear sizes in the chromatography system are large. Therefore for the *dynamics* the multicomponent X_n -concentration waves achieve the so called «coherent state»[26-30]. In the coherent state the X_n -multicomponent waves are separated by the concentration plateaus and move synchronously[26-33].

b) In the diffusion multicomponent MMT *kinetics* systems (like in the multicomponent NC *kinetics* considered here), the behavior of the $X_{nL(ro)r}(T)$ -waves and its interpretation differ in the presence of the diffusion phenomenon (even in the absence of the chemical reactions (I)). Due to the short ($L;ro,r$)-distances the propagation of the diffusion $X_{i,nL(ro)r}(T)$ -concentration waves takes place in the NC MMT kinetics systems without the formation of the concentration plateaus between the $X_{i,nL(ro)r}(T)$ -waves[1-9,22,23,25]. In this case, due to a limited small size (like: $L;ro,r$) of the various matrices the $X_{i,nL(ro)r}$ -concentration waves are unable to disperse with the formation of the concentration plateaus.

Therefore, the *coherent* state (or else the *stationary* state) might not be attainable in all NC&IEx kinetics variants of the MMT process due to the short distance covered by the X_n -waves in the MMT *kinetics* systems[16-18,20-23,25]. However, it is naturally that in the case of the MMT, NC(&IEx) kinetics, the effect of the interference of the multicomponent diffusion kinetic X_n -concentration waves takes place[1-9,16-18,22,23,25]. All the results of the computerized MMT, NC(or IEx) kinetics simulations show the essential meaning of the $X_{i,nL(ro)r}(T)$ -concentration waves interference in the course of time (T)[1-10].

One of the main result of the computerized modeling with the author's *bi-functional* NC Model approach is presented in S. 5. It has been shown that the basic properties of the NC, MMT kinetics process inside the multicomponent *bi-functional* NC system (NC $L;ro,r$ -distances) are *analogous* to the characteristics of the MMT dynamics process in the theory of chromatography (*see* Table 1, S. 5)[5-9].

5. NC, MMT kinetics. computerized simulation of the multi-component X_n -concentration waves behaviour

During the computerized modeling the numerical solution of the mass balance differential n-Eqs. (3.3) for the MMT, NC kinetics gives the multicomponent ordered numeric array of the $X_{i,nL(ro)r}(T)$ -dependences for the $X_{nL(ro)r}$ -concentration waves. Then the results of the mathematical finite differences solution-modeling should be *visualized* into the computerized pictures with the propagating multicomponent $X_{nL(ro)r}$ -concentration waves (distributions): $X_{nL(ro)r}(T^S)$ in the course of the discrete T^S -time moments.

The calculated $X_{nL(ro)r}(T^S)$ -concentration «waves» (expressed in the numerical tables) are necessary to transform («visualize») into the computerized calculated «pictures-frames» (the *visualization*), which illustrate quantitatively the propagation of the computed $X_{nL(ro)r}(T^S)$ -concentration waves in the course of T^S -time.

This illustration is visual and fairly good understandable. Then the calculated «pictures-frames» are assembled in the author's Scientific Computerized Animations: «SCA.avi» video files (see details and comments in S.3; S.6.2 also). The multi-colored «SCA.avi» files show clearly the propagation of the diffusion multi-component $X_{nL(ro)r}(T^S)$ -concentration waves for the n-components in the *bi-functional* NC L;ro,r -matrices for the NC MMT kinetics.

The problem of the *visualization* of the results of the computerized modeling for the MMT kinetics is solved successfully via the application of the visual multi-colored «Scientific Computerized Animations» video files («SCA.avi»). The author's multi-colored «SCA.avi» files have been generated after the process of the computerized simulation. The detailed description and estimations of the «multi-colored SCA» method with the «SCA.avi» theoretical applications and advantages are presented in the conclusive sections: S.5&S6(CONCLUSION).

Such type of the computerized *visualization*, i.e. transformation «multicomponent numeric array» → into the sequence of the «multi-colored pictures» gives the two possibilities for the study and for the presentations of the results:

a) the illustration of the study of the MMT kinetics via the visual distance-time pictures of the propagation of the $X_{nL(ro)r}(T^S)$ -concentration waves in the *bi-functional* NC (S.5) L;ro,r -matrices;

b) the further improvement of the presentation of the MMT kinetics process inside the NC (S.5) matrices via the construction of the multi-colored video file («SCA.avi») with its subsequent execution (during the oral presentations in the any sci. conferences and seminars).

Thus the obvious visual advantages of the *visualization* of the computerized results into the visual $X_n(\text{distance}; T)$ -concentration waves propagation on the basis of the multi-component waves W^+ -concept with the follow-up application are rather evident. The creature of the oral computerized presentations by the implementation of the multi-colored pictures showing the propagating multicomponent $X_n(\text{distance}; T^S)$ -concentration waves behavior with the additional attaching of the corresponding author's «SCA.avi» multi-colored video files are especially impressive. The execution of the multi-colored «SCA.av» animation video files permits the adequate perception of the propagation of the multicomponent $X_n(\text{distance}; T^S)$ -concentration waves. The visual travelling multi-colored $X_{nL(ro)r}(T)$ -profiles are demonstrated for the sci. audience in the course of T-time during the computerized oral lecture-presentation.

For the 5-component example (n=1,2-5; ₅Variant 1, S.5.1.1) there are presented in Figs. 3(a,up;b,down) & calculated Figs. 4(a,small K_S^1 ; b,large K_S^2) the movements of the $X_n(L,ro,r; T)$ -concentration waves.

The propagation of the $X_{nL(ro)r}(T^S)$ -waves in Figs. 4a,b($K_S^{1,2}$) includes the motion of the integral $CM_k^{L(ro)r}(T)$ -characteristic parameters: «triangles» on the abscissas: L(up); ro(middle),or r(down). The integral $kR_{L(ro)r}^0(T)$ -waves broadening during their propagation are characterized by the corresponding $Disp_k^{L(ro)r}(T)$ -time dependencies (dashed curves) which are presented below in the calculated Figs. 5a(small K_S^1), b(large K_S^2) for the two Selectivity $K_S^{1,2}$ -values.

The three $CM_k^{L(ro)r}(T)$ -time dependences for the integral $kR_{L(ro)r}^0(T)$ -concentration waves are also presented in the calculated Figs. 5a,b (solid curves). It is seen from Figs.

5a,b ($K_S^{1,2}$) that both integral (T-time dependent) characteristic parameters: $CM_k^{L(ro)r}$ (solids) & $Disp_k^{L(ro)r}$ (dashed) in Figs. 5a(left), b(right)) are determined essentially by the Selectivity $K_S^{1,2}$ -values ($K_S^1=36,a$) << $K_S^2=398,b$).

The multicomponent $X_{nL(ro)r}$ -waves propagation occurs to the *left* side (where $L;r,ro=0$) from the *right* side (where $L;r,ro,r=1$) of the $L;ro,r$ -matrices along the black arrow with the visual illustration in the Figs. 3(a,up;b,down)&calculated Figs. 4a,b($K_S^{1,2}$). The illustrations in Figs. 3a,b&Figs. 4a,b show additionally the computerized graphical pictures of the propagation of the integral $kR_{L(ro)r}^0$ -concentration waves which describe effectively and obviously the K_S -Selectivity influence in the computed Figs. 4a,b($K_S^{1,2}$).

The qualitative Figs. 3a(L-up);b(ro, r-down) in comparison with the two «computed» Figs. 4a,b($K_S^{1,2}$)(for $L;ro,r$ -distances) show the same NC kinetics process for the $X_{nL(ro)r}(T)$ -waves propagation along the three various ($L;ro,r$)-distances.

The movements of the all $X_{nL(ro)r}(T^{0,1,2}$ or $T^S)$ -concentration waves occur to the *left* sides from the *right* sides of the NC $L;ro,r$ -matrices (along the arrow's direction) in Figs. 3a(L),b(ro,r). In the computed Figs. 4a,b($K_S^{1,2}$) the same NC, MMT process occurs along the *L-up; ro-middle, r-down* (K_S^1,a),or (K_S^2,b) for the two various Selectivity values: *small* $K_S^1(a)$, or *large* $K_S^2(b)$.

5.1 Generalized example of the five (5) component System of the NC, MMT kinetics

Figures 3a(L,up), b(ro,r,down)&Figs. 4a,b($K_S^{1,2}$),(for $L;ro,r$), or the computed Figs. 5a,b($K_S^{1,2}$) demonstrate visually in the S. 5.1;5.2 the results of the computerized modeling for the generalized example of the 5-component ($_5$ Variant 1) MMT kinetics in the *bi-functional* NC $L;r,ro$ -matrices. These Figures 3-5 include the description of the behavior of the integral $kR_{L(ro)r}^0(T^S)$ -concentration wave (Figs.4a,b; $K_S^{1,2}$) with the $[kR^0]$ -concentrations of the «nanosites» (Figs. 1a,d; 2a,b). The example ($_5$ Variant 1) is represented by the $k(5)$ -component system with the one dissociation-association MAL_S Selectivity reaction (I.2) (conception scheme of the *bi-functional* NC, Figs. 2a,b)[3-9].

The computerized modeling for the example of the $_5$ Variant 1 describes the sorption of the n -components ($n \leq k=5$) of H_2SO_4 -acid including the integral $kR_{L(ro)r}^0$ -concentration waves behavior (*brown* color in Figs. 3a(L,up),b(ro,r,down), and in the computed Figs. 4a,b ($K_S^{1,2}$),(for $L;ro,r$ -distances) during the MMT, NC kinetics in the *bi-functional* NC $L;r,ro$ -matrices. For the $_5$ Variant 1 the list of the n -components (i,p -ions, including fixed k -component (kR^0), and m -component, $m(Rp)^+$) participating in the MMT NC kinetics process[5-9] inside the *bi-functional* NC $L;r,ro$ -matrices are presented in S.5.1.1 (*below*).

Figures 3a(L,up),b(ro,r,down) demonstrate visually the idealized qualitative illustration of the $_5$ Variant 1 with the propagation of the $X_{nL(ro)r}(T^{0-2})$ -concentration waves during the n -component NC, MMT kinetics process in the course of T-time: $T^0=0 < T^1 < T^2$.

The multi-colored illustrations in Figs. 3a(L-up),b(ro,r,down) facilitate the perception of the NC, MMT kinetics process of the n -components in the NC matrices, which is illustrated quantitatively and visually for the various NC $L;r,ro$ -matrices in the computed Figs. 4a,b ($K_S^{1,2}$) with distances: (*L-up, ro-middle, r-down*) for the two various $K_S^{1,2}$ (a,b) - Selectivity values.

For the L -membrane the propagation of the planar X_{nL} -waves occurs along the horizontal L -thickness (Figs.1d, S. 1). The direction of the X_{nL} -waves horizontal propagation is denoted by «black» \leftarrow arrows for the three figures: Figs.3a(L-up),b(ro,r,down), and the computed Figs. 4a,b ($K_S^{1,2}$); for *L-up; r-middle, r-down*.

For the (ro), r -matrices the propagation of the $X_{n(ro)r}$ -waves occurs along the radius (Figs.1a, and Figs. 3b(ro,r-down) & 4a,b($K_S^{1,2}$) for *ro-middle; r-down*. The «total ro,r – direction» of the $X_{nro,r}$ -waves propagation is denoted by the «black» \leftarrow arrows

(Figs.3b,*down*, and Figs.4a,b ($K_S^{1,2}$) for (ro),r-shapes). The two «black» \leftarrow arrows denote the same «(ro)r-direction» for the $X_{n(ro)r}$ -waves motion separately for the two various Selectivity $K_S^{1,2}$ -values: Figs. 4a,b($K_S^{1,2}$).

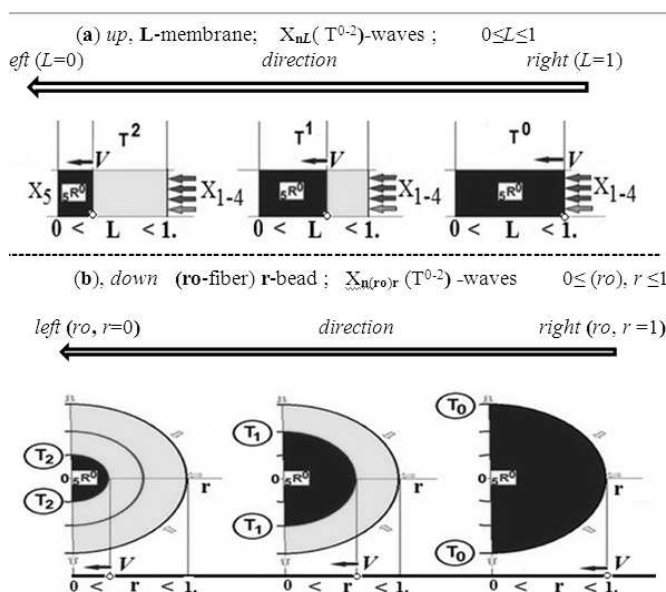


Fig. 3a(L,up);b($ro,r,down$). MMT, NC kinetics, five (5)-component. Conceptual qualitative explanation via illustrative ideal scheme. Propagation of X_{1-4} (yellow)& ${}_5R^0_{L(ro)r}$ (T^S)(brown)-concentration waves in course of time ($T^S=T^{0,1,2}$): (a) NC, L-membrane (cut); (b) NC (ro),r-matrices (cut of (ro-fiber); r-bead). Qualitative analog with an ideal illustration (propagation of X_n -waves) of MMT computerized modeling (presented in computed Figs. 4a,b). Mixture of X_{1-4} waves (yellow); integral ${}_kR^0$ -wave; $L,(ro)r$ -directions of $X_{nL(ro)r}$ -waves propagation along V -arrows: to left ($L,(ro)r=0$) \leftarrow from right ($L,(ro)r=1$). $T^S=T^0(0),T^1,T^2$; $n=1-4$; $5. 0 \leq L(ro)r \leq 1$.

The qualitative MMT, NC kinetic process in Figs. 3a,b is idealized: for the simplicity of the perception all the diffusion ($D_{i,j,p}=0$) effects are not included. For the simplicity of the perception the movement of the X_{1-4} concentration waves from the 5-component mixture is illustrated by the one («yellow») color in Figs. 3a($L-up$);b($ro,r-down$). The integral ${}_5R^0_{L(ro)r}$ -waves (brown color) are moving to the left ($L;r,ro=0$) in the course of $T^{0,1,2}$ -time without the diffusion «broadening» effects as in the ideal case: ${}_5R^0_{L(ro)r}$ in Figs. 3a($L-up$);b($ro,r-down$).

The real computed profiles of the $X_{(1-4)L(ro)r}$ -waves (colored four concentration profiles) including besides the integral ${}_kR^0_{L(ro)r}$ -wave (brown, solids profiles at $T^S=11$) are shown inside the *bi-functional* NC $L;(ro)r$ -matrices in the Figs. 4a,b($K_S^{1,2}$) (with the ${}_kR^0_{L(ro)r}$ -concentration waves moving to the left ($CL; ro,r=0$)[3-9].

Furthermore for the explanations it is used the obvious *analogy* between the qualitative ideal Figs.3a($L-up$),b($ro,r-down$) MMT process, and the computed (via the simulation) real MMT computed process in Figs. 4a,b($K_S^{1,2}$; $L-up$; $ro-middle, r-down$) for the adequate perception of the computed results of the MMT kinetics in the NC, $L;(ro)r$ -matrices obtained during the modeling in Figs. 4(a,b; $K_S^{1,2}$)[2-9]. Figures 3a(up),b($down$) &Figs. 4(a,b, $K_S^{1,2}$) show the propagations of the multicomponent $X_{nL(ro)r}$ -concentration waves which occur equally (with the exception of the broadening effects in the idealized Figs. 3a,b).

The five (5)-component (*5Variant 1*) *bi-functional* NC, MMT process (described via the I&II co-routes in Figs. 2a,b) in the *bi-functional* NC matrix (with the $5R^0$ -«nanosites», Figs. 1a,d) is accompanied by the two MAL_S relations: (one with minor influence) and another with the essential reaction (I.2) realizing the main Selectivity reaction (I.1), (I), co-route (Figs. 2a,b,*up* for the NC, MMT).

The additional diffusion co-route (II) is described by the three $\{D_{1SO_4}, D_{3HSO_4}, D_{4H}\}$ -multi-Diffusion, co-factor II (Figs.2a,b,*down*) for the three diffusible e(1,3,4)-components: Figs.4a,b ($K_S^{1,2}$) with the colored $X_{(1-4)L(ro)r}$ -waves & $kR^0_{L(ro)r}$ -waves (brown, $k=5$).

The integral $5R^0$ -wave propagation occurs as the effect of the two factors in the NC matrix:

I) the MAL_S (I.2) K_S -Selectivity reaction (I.1); (I, co-route; Figs. 2a,b & Figs. 4a,b $K_S^{1,2}$) with the «mass transformation» for the $p=4H^+$ -component, onto the kR^0 -«nanosites» (Figs. 1a,d) with the corresponding fixed k-component, ($D_k=0$), i.e. $p(4)H^+ + kR^0_m(RH)^+$;

II) the ($\{D_{1SO_4}, D_{3HSO_4}, D_{4H}>0\}$)-multi-Diffusion factors where the propagation of the $X_{4H}(p=4)$ concentration wave plays the key role (due to the combined behavior of the $p=4H$ -component-reactant: (I,co-route)& D_p -Diffusion(II,co-route) in pores (Figs.1a,d; 2a,b).

The «mass transformation», MAL_S (I.2) of the diffusible $4H^+$ -component ($p=4$) in the (I.1) reaction) together with the simultaneous D_{4H} -diffusion propagation of the $4H^+$ -concentration wave brings the change of the $[kR^0]$ -concentration distribution for the integral kR^0 -wave (S.3). Consequently the MAL_S (Selectivity) «mass transformations» (I.1), together with the combined $p(4H^+)$ -behavior (marked *above* in S.3) conditioned the propagation of the integral $kR^0_{L(ro)r}$ -concentration waves, (though the D_k -diffusivity is zero, i.e. $D_k=0$) for the *5Variant 1* in the computed Figs. 4a b ($K_S^{1,2}$).

The $Disp_k^{L(ro)r}(T)$, (Dispersion) T-time dependence describes the change of the effective width of the integral $5R^0_{L(ro)r}$ -concentration waves (in course of the discrete T^S -time) with the computerized calculations as in Figs. 4a,b($K_S^{1,2}$)&5a,b($K_S^{1,2}$) in correspondence with «the Dispersion» physical meaning.

Naturally there is the direct and clear coincidence mentioned between the NC kinetics processes depicted by the ideal qualitative Figs. 3a(*up*),b(*down*) and quantitative (computed) Figs. 4a,b ($K_S^{1,2}$). The straight comparison of the qualitative (Figs.3a(L),b(ro,r)&computed Figs.4a,b (for *L-up,ro-middle,r-down*) clarifies the entity of the MMT, NC kinetic process.

Thus due to the qualitative, ideal (Figs. 3a(L,*up*),b(r,*ro,down*)) and computed Figs. 4a,b($K_S^{1,2}$,*L-up (ro-middle)r-down*) modeling the propagation of the integral $kR^0_{L(ro)r}$ -concentration waves with the two integral characteristics (2x3 in the computed Figs.5a,b, $K_S^{1,2}$): $CM_k^{L(ro)r}$ -movement & broadening $Disp_k^{L(ro)r}$ for the integral $kR^0_{L(ro)r}$ -concentration waves is perceived visually and in full extent.

For the instant T^S -moment Figs. 4a,b ($K_S^{1,2}$; *L-up;(ro-middle),r-down*) show the calculated $X_{nL(ro)r}$ -concentration waves (*brown* profiles) which propagate (according to the scheme in Figs. 3a(L),b(ro,r)) in the course of T^S -time ($0 \leq T^S \leq 15$) during the computerized simulation (S.3) of the MMT process in the *bi-functional* NC L;(ro),r-matrices. The $CM_k^{L(ro)r}$ -positions are shown by the «triangles» on the abscissa: *L-up, ro-middle, r-down* for the two various Selectivity $K_S^{1,2}$ -values in Figs. 4a,b ($K_S^{1,2}$), where $K_S^1 \ll K_S^2$ [3-9].

The calculated (S.3) integral $5R^0_{L(ro)r}$ -concentration waves in the k(5)-component NC, MMT system (with the X_{1-4} -concentration waves, *5Variant 1*) are represented by the smooth curves of the integral $5R^0_{L(ro)r}$ -wave distributions (*brown, solids*) in Figs. 4a,b($K_S^{1,2}$). The integral $CM_k^{L(ro)r}(T)$ & $Disp_k^{L(ro)r}(T)$ -characteristics calculated in Figs. 5a,b($K_S^{1,2}$) are applicable (with the strong computerized estimation) to the integral $kR^0_{L(ro)r}$ -

waves behavior (for 5 Variant 1) considered as the wave profiles computed for the instant point of time ($T^S=11$) in Figs. 4a,b($K_S^{1,2}$).

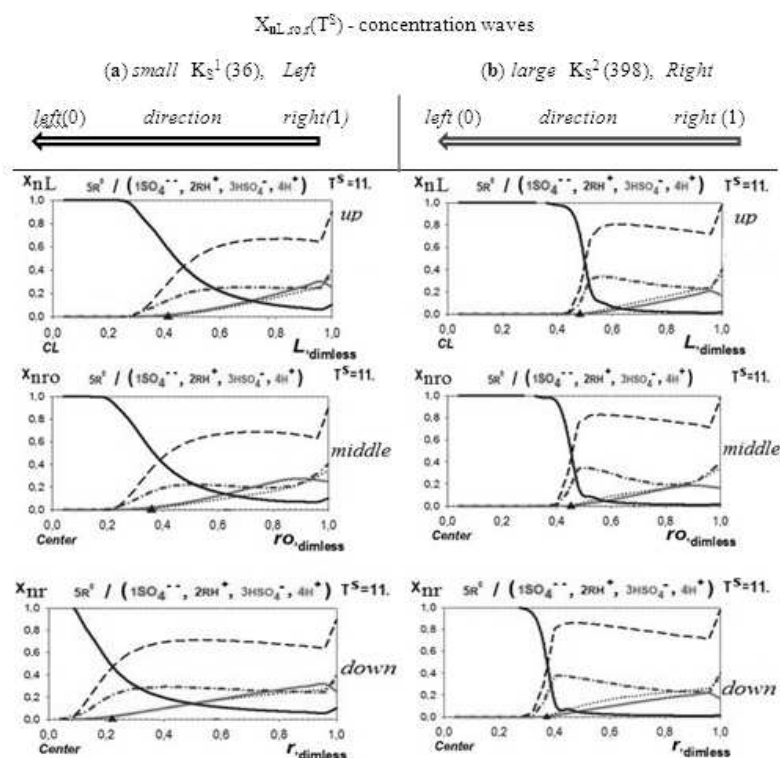


Fig. 4a(*small* K_S^1 , *Left*); b(*large* K_S^2 , *Right*). 5 Variant 1, $X_{nL(ro)r}$ -concentration waves for NC matrices. Five(5)-component NC, MMT system: anion $1SO_4^{2-}$ (red, dashed-dotted); $2RH^+$ (blue, dashed); $3HSO_4^-$ (green, dotted); $4H^+$ (pink, solid); integral $5R^0_{L(ro)r}$ -wave (brown, solid). Comparison of propagating integral $5R^0_{L(ro)r}$ -waves (with $D_5=0!$) in *bi-functional* NC matrices: L-membrane(*up*); ro-fiber(*middle*); r-bead(*down*). «Triangles» on (L ;ro,r)-abscissa show $CM_5^{L(ro)r}$ positions in NC L;ro,r-matrices. $D_{3HSO_4}=0.0085 < D_{1SO_4}=0.01 < D_{4H}=0.03$. Propagation along arrows.

Time moment ($T^S=11$): (a), $K_S^1(36) \ll K_S^2(398)$, (b).

Figures 4a,b($K_S^{1,2}$) represent the visual example (for the discrete T^S -time) one of the «frames-pictures» which compose (after assembling) the computerized, and multi-colored author's SCAnimation («SCA.avi» video files) mentioned. The SCA applications are described in the final S.6.2, Conclusions. The composed multi-colored «SCA.avi» video file presents the results of the modeling of the MMT, NC kinetics, i.e. the obvious visual propagation of the computed $X_{nL(ro,r)}(T^S)$ -concentration waves inside the *bi-functional* NC L;ro,r-matrices. The multicomponent computerized multi-colored «SCA.avi» video files method used by author have been characterized and discussed in the manuscript (S. 1,3, and finally in S.6.2).

The SCA video files («SCA.avi») constructed are used further for the introduction into the oral scientific presentations. The purpose of the multi-colored «SCA.avi» video file implementation is to demonstrate obviously and visually the results of the numerical multi-component calculations of the propagating ($X_n \& 5R^0$) $_{L(ro)r}$ -concentration waves during the computerized modeling of the MMT, NC processes[3-10].

On the basis of the wave W^+ -concept the propagation of the multicomponent $5R^0_{L(ro,r)}(T^S)$ -concentration waves for the MMT process in the NC L;ro,r-matrices is per-

ceivable easily by the sci. audience during the oral presentation of the propagation of the X_n & ${}_5R^0$ (distance; T^S)-concentration waves (including in particular the previous studies for the theory of multicomponent chromatography)[2,35,36] (for the examples see S.6.2).

For the example of 5-component MMT kinetics in the *bi-functional* NC matrices ($k=5$, ${}_5$ Variant 1, $L;ro,r$ -distances) the results of the numerical modeling are presented visually by the «frames-pictures» as in the example of Figs. 4a,b($K_S^{1,2}$) with the inclusion of the propagation of the smooth integral ${}_5R^0_{L;ro,r}$ -concentration waves together with the integral $CM_k^{L(ro)r}(T)$ & $Disp_k^{L(ro)r}(T)$ dependences in Figs. 5a,b($K_S^{1,2}$).

Besides it will be shown *below* (S.5) that there is very productive to use the combined approach based on the wave W^+ -concept together with the well-known «integral concept»[40] by using of the two integral $CM_k^{L(ro)r}(T)$ & $Dsp_k^{L(ro)r}(T)$ -parameters depending on T -time. These two statistical parameters[40] are calculated easily during the computerized numerical solution of the MMT n-Egs.(3.3) mentioned.

The integral $CM_k(T)$, $Disp_k(T)$ -parameters characterize effectively the behavior of the integral ${}_kR^0_{L(ro)r}(T^S)$ -concentration waves along the ($L;ro,r$)-distances in the course of the discrete time (T^S) during the simulation of the MMT processes. The (T)-time dependences in Figs. 5a,b($K_S^{1,2}$) describes the movement of the integral ${}_kR^0_{L(ro)r}(T^S)$ -waves along the $L;ro,r$ -distances in the NC matrices to the r,ro -Center, (and to the *left* side of the L -membrane, where $L;ro,r=0$).

These results of the computerized investigations[3-9] give the possibility to analyze and estimate the $X_{nL;ro,r}(T^S)$ -concentration waves behavior for the NC, MMT kinetics. The estimations concern especially the *analogy* for the ${}_kR^0_{L;ro,r}(T)$ -concentration wave behavior between the multicomponent NC, MMT sorption kinetics and the theory of multicomponent chromatography (MMT in filters, see Table 1 & CONCLUSIONS in S.6).

5.1.1 ${}_5$ Variant 1. Five (5)-component MMT NC kinetics: Sorption of H_2SO_4 -acid ions inside the bi-functional NC matrices

${}_5$ Variant 1. NC, MMT kinetics of H_2SO_4 -acid for 5-component *bi-functional* NC System.[5-8] The list of n-components (n-numbers, indices are placed here to the left of the n-Symbols) with the corresponding diffusivities D_n :

${}_1SO_4^{2-}$ -acid anions (sulphates); Diffusivity ($D_1=0.01$) in the NC pores, (Figs. 1a,d); II route, Figs. 2a,b);

${}_2(RH^+)$ -immovable 2^{nd} -component, $({}_2RH^+)$ -complex ($D_2=0$), formed by the ${}_kR^0$ -nanosites, by association with the acid cations (${}_4H^+$): Selectivity, reaction (I.1), (MAL_S I-route ${}_m(Rp)^+$, Figs. 2a,b); $m=2$; $p=4H$;

${}_3HSO_4^-$ -anion of acid (MAL -reaction (I.1;I.2); Diffusivity ($D_3=0.008$) inside the NC pores;

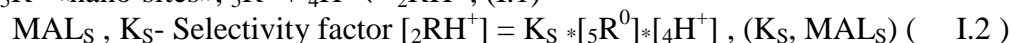
${}_4H^+$ -cations of H_2SO_4 -acid with the diffusivity ($D_{4H^+}=0.03$) in the NC pores (Figs. 1a,d);

${}_5R^0$ -zero valent, fixed nano-sites ($D_5=0$), I route, ; ${}_kR^0$ (Figs. 1a,d; 2a,b).

The MMT, NC system (I route: $Ia \rightarrow ; -Ib$) is characterized by $k=5$ components, three diffusion coefficients (in pores): D_{1SO_4} ; D_{3HSO_4} ; D_{4H^+} including the minor MAL_S reaction in the NC pores (see *above*), and the most important MAL_S «essential» Selectivity reaction (I.1) at the active ${}_5R^0$ «nanosites» (see Figs. 2a,b(*up*)).

The computerized numerical modeling shows that the influence of the MAL reaction in pores is minor (see S. 3), and therefore practically may not be taken into account in the theoretical consideration. Nevertheless in any case of the computerized modeling the MAL relations in pores are included into the author's *Fortran* computer programs designed.

The principal, main influence of the K_S -Selectivity factor for the calculated *bi-functional* NC, MMT kinetics is included via the MAL_S (I.2) Selectivity reaction (I.1) presented visually, and discussed in details in S.2 (conceptual scheme in Figs. 2a,b) reaction at the active ${}_5R^0$ -«nano-sites», ${}_5R^0 + {}_4H^+ \rightleftharpoons {}_2RH^+$, (I.1)



The MAL_S relationship in Eqs. (I.2) are presented by the MAL_S relation with the Selectivity K_S -constant. The K_S -factor (I.2), of the «association (Ia \rightarrow , forward)»-«dissociation (backward, \leftarrow Ib)» mechanism (Figs.2a,b,up) in the MAL_S reaction (I.1) is realized along the I,co-route, (Selectivity) via the introduced specific, key ${}_5R^0$ -«nanosites» component for the author's *bi-functional* NC Model (see above S. 2, conceptual scheme in Figs. 2a,b).

The creation of the author's SCAnimations (computer «SCA.avi» video files with the «*.avi» extension) for the NC, MMT kinetic process mentioned earlier (S. 3-5) is the best way to demonstrate the results of the computerized MMT simulation (via the numerical solution of the partial differential n-Eqs. (3.3)). (The details are presented in S.6, CONCLUSION).

5.2 MMT, NC Kinetics Process. Description via the integral ${}_kR^0$ -waves behavior in the *bi-functional* NC matrices

The results of the theoretical generalized numerical modeling are «calculated» on the basis of the author's elaborated novel *bi-functional* NC modern Model (S.2, 3)[1-9] by using the key concentration wave W^+ -concept. The numerical solutions approach includes the author's computerized modeling of the MMT, NC system with the solution of the partial differential n-Eqs. (3.3) including all the accompanying relations ((3.2-3.10) in S. 3).

The analysis and association of the qualitative figurative and visual explanation in Figs.3a(up),b(down) together with the computed Figs. 4(a,b, $K_S^{1,2}$) show the results of the computerized modeling of the NC, MMT kinetics for the 5-components system: (${}_1SO_4^{2-}$, ${}_2RH^+$; ${}_3HSO_4^-$; ${}_4H^+$; ${}_5R^0$) inside the NC matrices which contain initially (at $T=0$) only ${}_5R^0$ -«nanosites»(Figs. 1a,d), where the initial concentrations $[{}_5R^0]_{T=0}=1$, (Figs. 3a,b(ro, r); $T^0=0$).

At the first sight the integral ${}_k=5R^0$ -concentration wave is diffusion immovable in the NC matrices as the ${}_kR^0$ -component diffusivity is zero ($D_k=0$). However it is seen (in Figs. 4a,b) that the ${}_kR^0_{L(ro)r}$ -concentration waves propagate along the L,ro,r-distances to *left* ($L,ro,r=0$) from *right* ($L,ro,r=1$) along the black arrow.

The reason for the propagation of the ${}_5R^0_{L(ro)r}(T)$ -waves with the fixed k-component is presented *above* (S.3.1). The physical sense of the reason for the ${}_5R^0$ -wave propagation is in the «mass transformation» of the p-components (route I, Figs.2a,b) due to the MAL_S (I.2) Selectivity reactions (I.1) onto the ${}_kR^0$ -«nanosites» (see also S. 3.1;5.1).

There is shown the comparison of the propagating ${}_5R^0_{L(ro)r}(T)$ -concentration wave ($k=5$, *brown*, solids) with the comparative influences of the two $K_S^{1,2}$ -selectivity constant values in Figs. 4a,b($K_S^1=36$)&($K_S^2=398$). The integral ${}_5R^0_{L(ro)r}(T)$ -concentration wave propagates to the *left* ($L(ro)r=0$) for the small value ($a, K_S^1=36$) faster than for the *large* ($b, K_S^2=398$) value (in Figs. 4a,b): $CM_k^{L(ro)r}(K_S^1) < CM_k^{L(ro)r}(K_S^2)$.

For the dispersion ($Disp_k$) value the inequality is reverse (Figs. 5a,b): $Disp_k^{L(ro)r}(K_S^1, a) > Disp_k^{L(ro)r}(K_S^2, b)$. In other words the ${}_5R^0_{L(ro)r}$ -concentration waves propagate slower with the wave profile, which is sharper for the *large* K_S^2 -value (Figs. 4b, *Right*) in comparison with the ${}_5R^0_{L(ro)r}$ -concentration waves for the *small* K_S^1 -value (Figs. 4a, *Left*).

Besides, Figs. 4a,b illustrate (from *up* (L) to *down* (r)) the influence of the three various geometrical $L;r,o,r$ -shapes of the NC matrix on the integral ${}_5R^0_{L(ro)r}(T)$ -concentration waves (*brown*, solid) behavior for the two various K_S -values: (4a,b $K_S^{1,2}$).

Comparison of the propagating ${}_5R^0_{L(ro)r}$ -concentration waves in Figs. 4a,b (L -*up* ; r -*middle*, r -*down*) shows that for r -bead the integral ${}_5R^0_{L(ro)r}$ -waves is the fastest in the NC matrix than for two others NC shapes (L -membrane, and r -fiber), i.e. $CM_k^L(T) > CM_k^{ro} > CM_k^r(T)$. The corresponding comparison of the $CM_k^{L(ro)r}$ -positions in the pictures of Figs. 4a,b (from *up* to *down*) confirms the indicated inequalities. The same results for the various $L;r,o,r$ -shapes are even more obvious via the comparison of the $CM_k^{L(ro)r}$ -values for the $CM_k^{L(ro)r}(T)$ & $Disp_k^{L(ro)r}(T)$ -dependences in Figs. 5a(K_S^1) with 5b(K_S^2), and besides especially obvious and visual via the author's «*SCA.avi*» video files scanning.

Figures 5a(K_S^1 , *left*) & 5b(K_S^2 , *right*) illustrate especially clear the influence of the $K_S^{1,2}$ -Selectivity value in (I.2) for $CM_k^{L(ro)r}(T)$ & $Disp_k^{L(ro)r}(T)$, i.e. the increase of the K_S increases the completion time (T^{fin}) for the kinetic process: obviously that $T^{fin}(a, K_S^1) < T^{fin}(b, K_S^2)$.

The same joint general effects (reaction equilibrium (I, Selectivity) & (II, multi-Diffusion) are represented analogically in the theory of chromatography (in column filters) by the two terms also: multi-component isotherms for equilibria (*I*), and set of the broadening factors for the concentration waves in columns (*II*) (Table 1, *below*).

Factor (*II*) is described in the theory of chromatography by the habitual effective HETP_n -parameters for the chromatographic columns [1-5, 28-33]. The *analogy* of the two MMT (NC *kinetic* and IEx *dynamic, or chromatographic*) processes is summarized in the Table 1.

The Section 5 describes mainly the *5Variant* 1: MMT of the 5-components in the *bi-functional* NC matrix with the Selectivity, I association(Ia)-dissociation(Ib) MAL_S (K_S) reaction (I.1) onto the ${}_kR^0$ -«nanosites» (see the conceptual scheme, Figs. 2a,b in S.2). The influence of the first factor (co-route I, reaction (I.1), K_S -Selectivity factor) is determined by the K_S -Selectivity value: the more is $K_S^{1,2}$ the less is the $Disp_k$ of the integral ${}_5R^0_{L(ro)r}$ -concentration waves. In other words the width of the ${}_kR^0_{L(ro)r}$ -wave profiles becomes more narrowing (Figs. 5a,b($K_S^{1,2}$)) for the *large* (K_S^2) Selectivity value ($Disp_k$, dotted lines).

The same dependence for the ${}_kR^0_{L(ro)r}$ -wave widths (Figs. 4a,b, $K_S^{1,2}$) is obvious from the comparison of the widths for the ${}_kR^0_{L(ro)r}$ -waves in Figs. 4a($K_S^1=36$) & Figs. 4b(*large* $K_S^2=398$).

Besides, the comparison of the $CM_k^a(T)$ -curves (Fig. 5a, *left*, solids, $K_S^1=36$) for the *small* Selectivity (a) with the CM_k^b -curves (Fig. 5b, *right*, solids, $K_S^2=398$) for the *large* Selectivity (b) shows (from Figs. 5a, K_S^1 to Figs. 5b, K_S^2) that the more K_S -Selectivity is the slower is the ${}_5R^0_{L(ro)r}$ -concentration wave propagation. The same conclusion is followed from Figs. 4a,b ($K_S^{1,2}$) obviously (*brown* «triangles» on $L;r,o$ -abscissa, Figs. 4a,b).

It should be emphasized here the non-trivial, specific effect for the *bi-functional* NC system (marked previously in S.2,3): there is no diffusivity for the integral ${}_5R^0$ -component wave ($D_5=0$), nevertheless the propagation of the integral ${}_5R^0_{L(ro)r}$ -waves takes place (Figs. 4a,b($K_S^{1,2}$) & Figs. 5a,b($K_S^{1,2}$); see also Table 1).

The physical reason of such propagations is not the D_5 -diffusivity (as $D_{k=5}=0$) but the MAL_S «association-dissociation» reaction, (I.1) influence. All the effects bring the resulting mass transfer of the p -component (see *above*, S.2,3). It is conditioned consequently the propagation of the ${}_5R^0$ -concentration wave (Figs. 4a,b; $K_S^{1,2}$) of the fixed k -components. The remark concerning the combined p -component behavior (due to mass transformation in (I.1)) during NC, MMT process supports the previous conclusion (see also S. 2,3 above).

One more interesting result with the evidence of the above marked analogy can be seen from Figs. 5a,b. In these cases it takes place the typical behavior of the Dispersion, $\text{Disp}_k^{L(ro)r}(T)$ -parameter in the course of Time (T, abscissa) (which is known for the Dispersion due to the favourable isotherms in the theory of chromatography[26,32,33]).

The Dispersions, of the integral ${}_5R_{L(ro)r}^0$ -wave tend asymptotically ($\text{Disp}_k^{L(ro)r}(T)$ -dashed curves) to the permanent value (shown in Figs. 5a,b) at the end of T-abscissa (see the dashed curves behavior along the abscissa (T)).

The Dispersion curves- $\text{Disp}_k^{L(ro)r}(T)$ (dashed) behavior in Fig. 5a,b($K_S^{1,2}$) show visually, and distinctly the Selectivity effect for the Dispersions of the integral ${}_5R_{L(ro)r}^0$ -waves: $\text{Disp}_k^{L,ro,r}(T)$ values are narrowing with the asymptotic trend to the permanent $\text{Disp}_k^{L,ro,r}$ -values. (The influence of the second factor (II-multicomponent Diffusion) gives, as usual, the widening of the ${}_5R_{L(ro)r}^0$ -waves with the increase of the $\{D_{i,j,p}\}$ -multi-Diffusivity.)

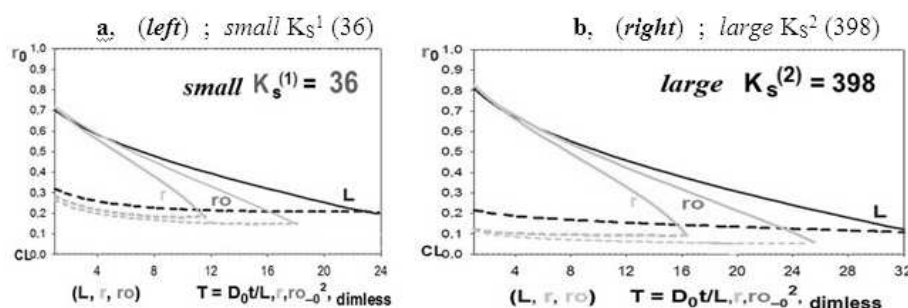


Fig.5a,(left); b,(right). ${}_5$ Variant 1: NC, MMT kinetics. Time (T) dependences for the integral parameters: $\text{CM}_5^{L(ro)r}(T)$, (solids); $\text{Disp}_5^{L(ro)r}(T)$, (dashed). Propagation of integral ${}_5R^0$ -concentration wave in *bi-functional* NC matrices: L-membrane (brown), ro-fiber (grey), r-bead (green). Ordinate axes: distance from matrix boundary ($L_0=r_0=r_0=1$) till «zero» point ($L=r_0=r_0=0$): $0 \leq r(\text{green}), ro(\text{grey}); L(\text{brown}) \leq 1$. $D_{\text{ISO}_4}=0.01$; $D_{\text{HSO}_4}=0.0085$; $D_{\text{H}}=0.03$. $T^{\text{fin}}(\text{b})=1.5 \cdot T^{\text{fin}}(\text{a})$; $K_S^{(1)}=36$ (a) $\ll K_S^{(2)}=398$ (b).

The reason of the differences in the ${}_5R_{L(ro)r}^0$ -waves propagation (Figs. 5a,b) is geometric: for the r-bead the diffusion occurs in the fewer volume in the course of time, T. For the ro-fiber the change in the volume ($\sim r dr$) for the multi-Diffusion is smaller (not so abrupt) than for an r-bead ($\sim r^2 dr$). For the L-membrane the change of the volume ($\sim dL$) for the multi-Diffusion of the planar L-wave is linear. In Figures 5a,b ($K_S^{1,2}$) the dependencies for the integral parameters: $\text{CM}_k^{L(ro)r}(T)$, (solids) & $\text{Disp}_k^{L(ro)r}(T)$, (dashed) are presented visually for the integral ${}_5R_{L(ro)r}^0$ -wave (${}_5$ Variant 1, with $D_5=0$) for the various shapes of the *bi-functional* NC matrices: L-membrane; ro-fiber, r-bead.

Figures 5a,b($K_S^{1,2}$) represent the time dependent estimations of the MMT, NC kinetics for the three various $L(ro)r$ -shapes of the *bi-functional* NC. The completion time (T^{fin}) of the kinetic process corresponds to the criterion: the amount of sum ($\text{CM}_k + \text{Disp}_k$) $^{L,ro,r}=1$. It means, that the distance covered by the integral ${}_5R^0$ -concentration wave to the moment T^{fin} is equal to the length of the matrix: L_0 (thickness), ro_0 (radius of cylinder) or r_0 (radius of sphere)[6-8].

In other words the completion time- T^{fin} corresponds to the «crossing» of the two curves (with the same color) in Figs. 5a,b($K_S^{1,2}$): $\text{CM}_k^{L,ro,r}(T)$, (solids) with $\text{Disp}_k^{L,ro,r}(T)$, (dashed). In accordance with this criterion of «crossing» [6-8] it is obvious from the both Figs. 5a,b($K_S^{1,2}$) that for any conditions the kinetic MMT process in the NC L,ro,r -matrices is the fastest one inside the r-bead and the slowest one inside the L-membrane.

The ro-fiber has the intermediate position in this row: $T_r^{\text{fin}} < T_{ro}^{\text{fin}} < T_L^{\text{fin}}$ (compare also the pictures in Figs. 4 a,b ($K_S^{1,2}$)[5-8].

The conclusions, and the relations are obvious and follow visually from the comparison in time (T) for Figs. 4a,b($K_S^{1,2}$). The relations ($T_r^{\text{fin}} < T_{ro}^{\text{fin}} < T_L^{\text{fin}}$) are especially evident from Figs. 5a,b($K_S^{1,2}$). The computerized simulation of the MMT kinetics inside the *bi-functional* NC matrix (S. 5) discovers the clear *analogies* of the multi-component NC kinetics[2-7] with the main theoretical basis of the theory of nonlinear multi-component chromatography[26-33].

Table 1. *Analogy* for MMT processes: (1), NC kinetics & (2), Theory of chromatography

(1) ~ (2): ANALOGY, MMT, WAVES (W^+) (1) NC MODEL, KINETICS ~ (2) THEORY of CROMATOGRAPHY (DYNAMICS)			DIFFERENCES, & FEATURES X_n - CONCENTRATION WAVES PROPAGATION
(1) MMT KINETICS BI-FUNCTIONAL NC MODEL	(1) EQUILIBRIUM REACTION Selectivity (I, K_S , MAL_S)	(1) NC MODEL , MMT WAVES DISPER- SION Multi - DIFFUSION { $D_{i,j,p}$ }, II	(1) MOVEMENT of ALL WAVES Includes: kR^0 , $m(Rp)^+$ - waves Though Diffusivities D_k , $D_m = 0$
(2) MMT DYNAMICS, THEORY of CHROMATOGRAPHY	(2) SORPTION EQUILIBRIUM (I) (Set of Isotherms)	(2) THEORY of CRO- MATOGRAPHY BROADENING WAVES DISPERSION HETP _i Effect (II)	(2) MOVEMENT of ALL WAVES (HETP _i + SORPTION + + MOBILE PHASE)

These *analogies* concern the multi-component ${}_5R^0_{L,ro,r}$ -concentration waves behavior in the *bi-functional* NC matrix[1-9].

The physical sense meaning of the reasons for the explanation of the propagating X_n (distance; T)-waves behavior (Figs. 4a,b ($K_S^{1,2}$) & Figs. 5a,b($K_S^{1,2}$) is described by the joint influence of the two co-working (I&II) factors: Selectivity,(I) & multi-Diffusion,(II) with the conceptual schemes in Figs. 2a,b (S.2).

In the theory of chromatography the same effect for the Dispersion takes place for the X_n -concentration waves, when the favorable isotherm factor (I) used to compensate the un-favourable influence of the broadening HETP factors (II) for the concentration waves (profiles) in columns: i.e. *favourable* equilibrium (I) *compensates* the widening of the X_n -waves with the same type of the asymptotic tendency for the dynamic wave's Dispersion[26,28-33].

5.3 Discussion. Results of Computerized Modeling of NC, MMT Kinetics

The modern author's NC *bi-functional* Model for the MMT kinetics process in the novel NC materials has been created[1-9]. The property of the *bi-functionality* of the NC Model supposes the two co-working I&II-routes for the NC, MMT kinetics process: the «mass transformation» (I.1;I.2) for the p,k,m-components (I, Selectivity, K_S -constant) & multi-Diffusion (II, { $D_{i,j,p}$ }) MMT kinetics is specified. The details of the author's *bi-functional* (co-routes I&II) NC Model are described in S.2 (Figs. 2a,b) of the manuscript.

The corresponding NC *bi-functional* Model elaborated is implemented into the computerized modeling of the nonlinear multi-component *bi-functional* NC, MMT systems (S.3). The numerical mathematical computerized solution of the MMT partial differential n-Eqs. (3.3, S.3) brings the new results describing the behavior of the multicomponent

$X_{nL(ro)r}$ -concentration waves propagating and interfering in the *bi-functional* NC matrices for the three various NC shapes: L-membrane, ro-fiber, or r-bead (S.5). There are obtained the corresponding conclusions concerning co-influence of the two MMT co-routes (I&II) inside the *bi-functional* NC matrices (conceptual Figs. 2a,b).

The quantitative estimations of the $X_n(L,ro,r; T)$ concentration waves behavior are obtained by using the two integral parameters: $\{(CM_k) \& (Disp_k)\}$ (S.5) characterizing the integral ${}_5R^0_{L(ro)r}$ -wave distributions for the k-component (${}_kR^0$ -«nanosites» with $[{}_kR^0]$ concentrations).

The larger is the main Selectivity MAL_S parameter (K_S) in relation (I.2) the steeper is the integral ${}_kR^0_{L(ro)r}$ -concentration frontal wave in the NC L;ro,r-matrices (${}_{k=5}Variant\ 1$, computed Figs. 4a,b($K_S^{1,2}$)). The behavior of the generalized width ($Disp_k$) of the integral ${}_kR^0$ -wave is described by the same rule as in the theory of chromatography: in the course of T-time the $Disp_k$ tends asymptotically (for $K_S > 1$) to the constant $Disp_k^0$ -value (Figs. 5a,b, dashed lines). This final $Disp_k^0$ -value depends on the MAL_S Selectivity factor (co-route I, K_S) with the multi-Diffusivity (co-route II, $\{D_{i,j,p}\}$)-values. The *analogy* just mentioned between NC, MMT kinetics and theory of MMT in multicomponent chromatography is marked in details in the Table 1 (S.5).

The key productive concentration wave W^+ -concept (S.4) is used in the mathematical multicomponent computerized simulation. The W^+ -concept brings the clear, effective and understandable treatment of the MMT, NC kinetics process in the *bi-functional* NC matrices of the various shapes: L-membrane, ro-fiber, r-bead (Figs. 4a,b&5a,b); $K_S^1(a) < K_S^2(b)$, S.5).

The multi-component concentration «wave» W^+ -concept is very effective in the study of the MMT, NC kinetics in the *bi-functional* NC matrices with the two determining factors: 1) MAL_S reaction (I co-route, I.1;I.2) onto the active ${}_kR^0$ -«nanosites» (K_S , Selectivity) including in addition 2) the co-route II, ($\{D_{i,j,p}\}$, multi-Diffusion) in the pores of the NC L;ro,r-matrixes (Figs. 1a,d ; 2a,b).

The understandable and visual treatment of the multicomponent propagating, and interfering $X_{nL(ro)r}(T)$ -concentration waves behavior during the MMT process becomes possible for the NC, MMT kinetics inside the L;r,ro-matrices. The influence of the two crucial factors: Selectivity (K_S , co-route I) & multi-Diffusion ($\{D_{i,p}\}$, co-route II) is demonstrated visually and well perceivable via the scanning of the author's «multi-colored «Scientific Computerized Animations (SCA.avi - video files) described detailed in the final Section 6.2.

6. Conclusions

The new generalized theoretical (computerized modeling) results of the MMT kinetics in the *bi-functional* NC r,ro,L-matrices (S.5) are determined by the interference of the propagating multicomponent $X_{n(i)}$ (distance; T)-concentration waves on the basis of the fundamental key wave, W^+ -concept. The wave W^+ -concept unites all the three subjects of the theoretical investigations in the manuscript: (a) MMT, NC kinetics (S.5 with 6.1 Conclusions); and (b) *Visualization* of the MMT NC kinetics (S.1,3,5; with S. 6.2, Conclusions).

6.1 Selective MMT kinetics in the bi-functional (I, K_S ; II, $\{D_n\}$) NC matrices

A. The computerized propagating X_n (distance; T)-concentration waves behavior is determined by the decisive influences of the two characteristic parameters combined inside the NC matrices:

I. MMT co-route (I) with the equilibrium parameters of the MAL_S reaction (Selectivity, K_S);

II. MMT co-route (II) with the multicomponent $\{D_n\}$ -multi-diffusion effects during the NC, MMT kinetics process. The marked analogy (in Table 1, S.5) of the multicomponent X_n (T)-concentration waves behavior is assigned consequently, in the analysis (S.5) to the both MMT cases: (1) the *bi-functional* NC, MMT kinetics, and (2) theory of multicomponent chromatography.

B. The propagation of the integral and specific kR^0 -concentration wave in the *bi-functional* NC matrix of the R^0 -«nanosites»(Figs. 1a,d) takes place, although the corresponding D_k -diffusivity is zero ($D_k=0$, Table 1, S.5).

Such atypical (*unusual*) concentration kR^0 -concentration wave behavior has the clear physical meaning. The diffusion propagation of the integral kR^0 -wave is determined by the “dual” behavior of the p-component which includes the combined p-participation in the two co-operative processes: i.e. in the p-«mass transformation» (via the co-route I) in the combination with the multi-Diffusion in the NC pores (via the co-route II, $D_p>0$, Figs. 2a,b). The corresponding conceptual scheme (Figs. 2a,b; S.2) displayed distinctly the combination of the two (I&II) co-routes.

6.2 Visualization of the results by the author's SCAnimations («SCA.avi») method

The variants (S.5) of the MMT kinetics processes inside the NC(in S.5) r,ro,L-matrices with the new theoretical results are visualized and provided obviously by author via the contemporary method of the *visualization* of the results of the computerized modeling, i.e.via the multi-colored computerized calculated SCA animations: the «SCA.avi» video-files.

The computerized «SCA.avi» video files are assembled (by the author) sequentially via the separate «frames» (arranged in course of T-time for the MMT process): «pictures» (as in Figs. 4a,b for NC) in the usual «animation pattern». The computerized SCAnimations scanning are executed via the «SCA.avi» multi-colored video files. For the manuscript considered the computerized SCAnimations demonstrate the propagation of the multi-component (& «multi-colored») $X_{n(i)}$ -concentration waves in spatial coordinates (L,ro,r-distances) in the course of T-time during the MMT kinetics processes inside the (*bi-functional* NC) r,ro,L-matrices.

Such multi-colored calculated SCAnimation (*SCA.avi*) video demonstrations of the MMT processes during the oral computerized presentation (at many international conferences in particular) are well perceived and understandable by the sci. audience. The SCA method has been used permanently for the implementation of the «SCA.avi» into the various oral thematic presentations by the author of the manuscript during a long-continued period of time (more than 14 years) for the demonstration of the results of the presented theoretical studies (on the basis of the fundamental key wave W^+ -concept) in the multi-component kinetics & dynamics (chromatography) of the MMT systems[2,34-36].

SCAnimations (as the prepared «SCA.avi» video files) have been used by the author with the permanent experience in the effective and visually perceptible presentations of the MMT kinetics (and dynamics) processes[2-9,34-36] in many International Conferences (including in particular the Conferences «IEX 2004, 2008, 2012», Cambridge, UK[2, 35,36]). The interferences of the X_n -concentration waves have been shown visually during the MMT dynamics and kinetics by the author's multi-colored SCA animations («SCA.avi») for a number of the International Conferences and seminars.

The visual demonstration of the *bi-functional* NC, MMT kinetics are prepared via the «SCA.avi»(video files) as the results of the computerized mathematical modeling with

the propagating and calculated $X_{n,i}$ -concentration multi-colored profiles-waves obtained for the successive time (T^S) moments[2,35,36].

References

1. Kalinitchev A, *Prot. Met. Phys. Chem. Surf.*, 2011, 47 (6), 698-706. (Site Springer : <http://www.springerlink.com/openurl.asp?genre=article&id=doi:10.1134/S2070205111060062>).
2. Kalinitchev A, Mass Transfer Kinetics Modeling in Bi-functional Ion Exchangers with Chemical Reactions on Active Centers. in *IEX2012*, ed: M. Cox, Society of Chemical Industry, London, S. Fundam. p 1-18, (2012). e-book (*The Intern. IEx 2012 Confer.* Thesis: p. 123-124).
3. Kalinitchev A, *Smart NanoComposites*. Nova Sci. Publ., Ed. (in Chief.:K.Levine), 2013, 3(2),pp.1-18. (Site:http://www.novapublishers.com/catalog/productinfo.php?products_id=40111).
4. Kalinitchev A, *Advances in Nanoparticles*. AnP.Sci.Res.Publ. : SCIRP. E-Journal., 2013, 2(2), pp. 1-18. (Site ANP: <http://www.scirp.org/journal/anp/>).
5. Kalinitchev A, *Prot. Met.&Phys. Chem. Surf.* (Springer Ed.), 2013, 49(6), 627-638. (Site Springer: <http://www.springerlink.com/openurl.asp?genre=article&id=doi:10.1134/S2070205113060051>).
6. Kalinitchev A, *Sorbtsionnye i khromatograficheskie protsessy*, 2013, Vol. 13, No 6, pp. 413-428.
7. Kalinitchev A, *NanoTechnol Rev (NTREV)*. Special issue (N5) "NanoTechnology: from Convergence to Divergence", DeGruyter Ed. 3(5):467-498 (2014). <http://degruyter.com/new/ntrev2014.3issue-files>.doi:10.1515/ntrev-2014-0007. Publ. on line 8.10.2014 (Ed. Ja S. Lee). NTREV(2014).
8. Kalinitchev A, *Prot. Met.&Phys. Chem. Surf.* (Springer Edition), 2013, 49 (6), pp. 627-638 Site Springer :<http://www.springerlink.com/openurl.asp?genre=article&id=doi:10.1134/S2070205113060051>);
9. Kalinitchev A, *Universal Journal of Physics and Application*, 2013, 1(2), pp. 130-143. Doi: 10.13189/ujpa.2013.010213.
10. Kalinitchev A, *Protection of Metals & Physical Chemistry of Surfaces, 2015*, 51(3), pp. 317-329. © Pleiades Publishing, Ltd. doi: 10.1134/S2070205115030119.
11. Kravchenko T, Polyansky L, Khorolskaya S, Kalinitchev A, , in *IEx2012*, ed: M. Cox, Society of Chemical Industry, London, 2012, pp. 1-15, (2012), e-book;(The Intern. IEx Confer., thesis: p. 113-114).
12. Kiprianova E, Kravchenko T, Konev D, Kalinitchev A et al., *J. Rus.Physical Chem.*, 2010, 84(6), pp. 1104-1110. DOI:10.1134/S003602441006018X
13. Kravchenko T, Polyansky L, Kalinitchev A., Konev D, *Nano Composites Metal - Ion Exchangers*. M. "Nauka"("Sci.") Ed. (2009). 390 p
14. Haase R, *Thermodynamics of Irreversible Processes*. Ch.2;4. M.: "Mir" Ed. (1967). 544 p.
15. Helfferich F, *Ion Exchange*. Mc.Graw-Hill. NY. Ch.6. (1962). (*Ionen Austausch*, Verlag Chemie, GMBH, (1959), Deutsch).
16. Helfferich F, Ion Exchange Kinetics. Ch.5. in *Ion Exchange* (A series of Adv.) ed. Ja.I. Marinsky). St. Univ. NY. , 1 (1966).
17. Helfferich F, Ion exchange kinetics - evolution of a theory. in: "Mass Transfer & Kinetics of IEx" (ed: L.Liberti&F.Helfferich) M.Sijthoff & Nordhoff . The Hague. 157-179 (1983), doi:10.1007/978-94-009-6899-8_6 .
18. Petruzelli D, Helfferich F, Liberti L, Millar J. et al., *Reactive Polymers*, 1987, 7, pp. 1-13.
19. Kalinitchev A., Kolotinskaya E., Semenovskaya T., *J.Chromatogr.*, 1982, 243, pp. 17-24.doi:10.1016/S0021-9673(00)88159-5.
20. Helfferich F, Hwang Y-I, *Am. I. Ch.E. Symp. Ser.*, 1985, 81, pp. 17-27.
21. Hwang Y-I, Helfferich F, *Reactive Polymers*, 1987, 5, pp. 237-252.
22. Yoshida H, Kataoka T, *J. Ind. Eng. Chem. Res.*, 1987, 26(6), pp. 1179-1184.
23. Yoshida H, Kataoka T., *J. Chem. Eng*, 1988, 39, pp. 55-62.
24. Dolgonosov A., Khamisov R., Krachak A., Prudkovskiy A, *React. Func. Polymers*, 1995, 28, pp. 13-20.
25. Kalinitchev A, Investigation of intraparticle IEx kinetics in selective systems, in (eds.: Ja. Marinsky & Y.Marcus) *IEx & Solv. Extr.* 12, M.Dekker, Ch.4:149-196 (1995).
26. Helfferich F., Klein G, *Multicomponent Chromatography. Theory of Interference*, New York: M. Dekker Inc., 1970., 360 p.

27. Helfferich F, Coherence : Power and Challenge of a new Concept. *New direction in Adsorption Technology*. G.Keller ed., Butterworth. Boston.1989, pp. 1-11.
28. Industrial & Engineering Chemistry Research. J. (*F. Helfferich Festschrift*), *J.Am.Chem.Soc.*34:2551-2922(1995). doi:10.1021/ie00047a029.
29. Tondeur D., Bailly M, *Chem. Eng. Process*, 1987, 22, pp. 91-105. doi:10.1016/0255-2701(87)80035-1.
30. Tondeur D, *Ind. & Eng. Chem. Res.*, 1995, 34, pp. 2782-2788. doi:10.1021/ie00047a029.
31. Hwang YL, *Ind.&Eng.Chem.Res.*, 1995, 34, pp. 2849-2864. doi:10.1007/978-94-009-85797:10.1021/ie00047 a039,
32. *Percolation Process: Theory and Applications*. ed.: Rodrigues, AE, Tondeur, D, The Hague: Sijthoff & Nordhoff, (1981). doi:10.1007/978-94-009-8579-7.
33. Kalinitchev A, *J. Rus. Chem. Reviews*, 1996, 65, pp. 95-115. doi:10.1070/RC1996v065n02A BEH000201.
34. Hoell W., Kalinichev A, *J. Rus. Chem. Reviews*, 2004, 73, pp. 351-370. doi:10.1070/RC2004v073n04ABEH000768.
35. Kalinitchev A., Hoell W, *IEX2004, Ion Exchange Technology for Today and Tomorrow*, ed:M. Cox, Society of Chemical Industry, London, 2004, pp 53-58.
36. Kalinitchev A., Hoell W, *IEX2008, Recent Advances in IEx Theory&Practice*, ed:M.Cox, Society of Chemical Industry, London, 2008, pp. 85-93.
37. Courant R., Friedrichs K, *Supersonic flow and Shock Waves*, Springer, 1999, 464 p.
38. Prigogine I., Herman R, *Kinetic Theory of Vehicular Traffic*, NY.:Elsevier, 1971, 55 p.
39. Whitham G, *Linear and Nonlinear waves*, Wiley. NY, 1974, 636 p.
40. Korn G., Korn T, *Mathematical Handbook*, Ch.18,19.McGraw-Hill,NY-Sidney, 1968.

Калиничев Анатолий Иванович –д.х.н. (физ. химия), гл. научный сотрудник Института физ химии и электрохимии им. акад. А.Н. Фрумкина РАН, Москва.

Kalinitchev Anatoliy I. – Doctor Habilitat (Phys. Chem.), principal investigator, Institute for Phys Chemistry and ElectroChemistry named after acad. A.N. Frumkin. RAS (Moscow). E-mail: [kali-na@phych.ac.ru](mailto:kalina@phych.ac.ru)